Atom-Light Interactions

M. P. A. Jones
E-mail: m.p.a.jones@durham.ac.uk

Course Aims

The aims of this section of the graduate course are (1) to familiarise you with some of the theory underpinning modern atomic physics experiments (2) to apply this framework to your own research.

Course Structure

The course consists of 8 lectures, with one lecture each week (9am Tuesday, Sir James Knott Room). The lectures will take the form of tutorial style discussions of the previous week's homework and key points from the notes. The course notes are available here; you will be expected to bring your own copy to the lectures.

Course Outline

Here I have broken down the course content into seven sections, roughly corresponding to the lectures. Towards the end of the course the lectures will become more like tutorials as we also discuss the previous weeks homework etc. the final lecture has been reserved for further analysis of the material we have covered.

1. **The density matrix** Including spontaneous emission. The density matrix and density operator. Master equations.
2. **The optical Bloch equations** Form of the equations. Steady-state solutions. Time-dependent solutions and the Bloch sphere.
3. **Relating microscopic and macroscopic properties**. Doppler broadening, susceptibility, absorption and refractive index.
4. **The three-level atom** Optical pumping, Raman transitions and electromagnetically induced transparency.
5. **Basic atomic structure**. Revision of basic atomic structure, fine and hyperfine splittings. Comparison of one and two electron atoms.
6. **Atoms in static electric and magnetic fields** Nature of the coupling of atoms to electromagnetic fields. Multipole expansion; the role of spin. Selection rules.
7. **Angular momentum operators and matrix elements** Techniques for solving problems in atomic structure and atom-field interactions.
8. **Angular problems in the uncoupled basis** This section develops techniques for solving angular problems in the uncoupled basis using matrix methods.

Core references

- Atomic structure and atoms in external fields: This material is well covered in *Elementary Atomic Structure* by Woodgate and *Physics of atoms and molecules* by Bransden and Joachim.

- Atom-light interactions: Key books are *The Quantum Theory of Light* by Loudon, and *Atom-photon interactions: Basic processes and applications* by Cohen-Tannoudji, Dupont-Roc and Grynberg.

1 The two-level atom

In the first part of the course we will develop the detailed theory of a two-level atom coupled to a classical light field, using the electric dipole approximation. The treatment we will use is adapted to intense, monochromatic radiation such as that produced by lasers, where, as we shall see, coherent effects need to be taken into account. We will develop the theory for a completely coherent interaction with the light field first, before introducing the density matrix and spontaneous emission. We will then look at resonance fluorescence and absorption. Finally we will look at extending the treatment to three-level atoms interacting with two light fields.

1.1 Atom light interactions in the Schrödinger picture

The two level atom is illustrated in Fig. 1. The atom has a ground state g and an excited state e, and the two states are coupled by an electric dipole transition of frequency ω_0. The atom interacts with a monochromatic radiation field of frequency ω, which can be detuned by an amount $\Delta = \omega - \omega_0$ from resonance.

The evolution of this system is governed by the time-dependent Schrödinger equation

$$i\hbar\frac{\partial\Psi(\mathbf{r},t)}{\partial t} = \hat{H}\Psi(\mathbf{r},t) \tag{1}$$

The atomic wavefunction at any time t can be written

$$\Psi(\mathbf{r},t) = c_g(t)|g\rangle + c_e(t)|e\rangle e^{-i\omega_0 t} \tag{2}$$

and the Hamiltonian is $\hat{H} = \hat{H}_0 + \hat{V}$, where $\hat{H}_0$ is the Hamiltonian of the unperturbed atom with eigenstates $|g\rangle$ and $|e\rangle$, and $\hat{V} = \hat{d}\cdot E$.

Substituting 2 into 1 yields two coupled differential equations for the coefficients $c_g(t)$ and $c_e(t)$

$$i\hbar\frac{dc_g(t)}{dt} = c_e\langle g|\hat{d}\cdot\hat{E}|e\rangle e^{-i\omega_0 t} \tag{3}$$

$$i\hbar\frac{dc_e(t)}{dt} = c_g\langle e|\hat{d}\cdot\hat{E}|g\rangle e^{+i\omega_0 t}. \tag{4}$$

For a plane wave, the electric field can be written as $\hat{E} = \hat{\epsilon}E_0\cos(k\mathbf{r}-\omega t)$. Substituting this into the equations 3 and 4 leads us to the definition of a key parameter for atom light interactions. The **Rabi frequency**

$$\Omega = \frac{E_0}{\hbar}\langle e|\hat{d}\cdot\hat{\epsilon}|g\rangle \tag{5}$$

describes the strength of the coupling between the atom and the electric field. It increases with increasing intensity, and for a given intensity it is dependent on the atomic states and the polarization through the dipole matrix element.

The coupled equations 3 and 4 can now be written as

$$i\hbar\frac{dc_g(t)}{dt} = c_e\hbar\Omega^*\left(\frac{e^{i(\omega-\omega_0)t}+e^{-i(\omega+\omega_0)t}}{2}\right) \tag{6}$$

$$i\hbar\frac{dc_e(t)}{dt} = c_g\hbar\Omega\left(\frac{e^{i(\omega_0+\omega)t}+e^{-i(\omega-\omega_0)t}}{2}\right). \tag{7}$$

where we have used the exponential form of $\cos(\omega t)$. Up to this point, the treatment, within the approximation of only two energy levels, has been exact. We now make an important approximation that is known as the **Rotating Wave Approximation**. We assume that terms like $e^{-i(\omega+\omega_0)}$ that oscillate at roughly twice the frequency of the driving field can be eliminated, as their time dependence averages out over the much slower timescale of the evolution of the coefficients c_g and c_e. This

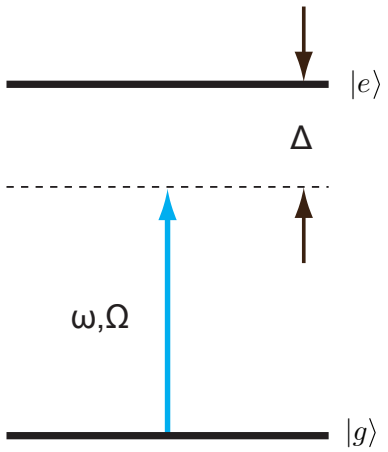

Figure 1: The two-level atom. The two energy levels are separated by a transition with frequency ω_0. The atom is driven by a monochromatic plane wave of frequency Ω. Two key parameters govern the dynamics of the atom-light interaction - the detuning $\Delta = \omega - \omega_0$ and the Rabi frequency Ω which describes the strength of the atom-field coupling.

approximation is routinely made, and it is a good approximation close to resonance, and if the driving is weak ($\Omega \ll \omega$).[1]

Retaining only terms like $e^{i(\omega-\omega_0)t}$, we introduce the other key parameter for atom-light interactions: the **detuning** $\Delta = \omega - \omega_0$ which, along with the Rabi frequency, will control the time evolution of this system. The two coupled equations can now be written

$$i\hbar\frac{dc_g(t)}{dt} = c_e\hbar\Omega^*\frac{e^{i\Delta t}}{2} \tag{8}$$

$$i\hbar\frac{dc_e(t)}{dt} = c_g\hbar\Omega\frac{e^{-i\Delta t}}{2}. \tag{9}$$

The easiest way to solve these equations is to differentiate again with respect to t which yields the following pair of (uncoupled) equations for the coefficients:

$$\frac{d^2c_g}{dt^2} - i\Delta\frac{c_g}{dt} + \frac{\Omega^2}{4}c_g = 0 \tag{10}$$

$$\frac{d^2c_e}{dt^2} + i\Delta\frac{c_e}{dt} + \frac{\Omega^2}{4}c_e = 0 \tag{11}$$

1.1.1 Rabi oscillations

If we assume that at $t = 0$, $c_g = 1$ and $c_e = 0$, then equations 10 and 11 can be solved to give the following expression for the probability to be in the excited state $|c_e(t)|^2$:

$$|c_e(t)|^2 = \frac{\Omega^2}{\Omega'^2}\sin^2\left[\frac{\Omega' t}{2}\right] \tag{12}$$

where $\Omega' = \sqrt{\Omega^2 + \Delta^2}$. The probability to be in state $|e\rangle$ undergoes *Rabi oscillations* at frequency Ω', as shown in Fig. 2. On resonance, a pulse of duration $T = \pi/\Omega$ is known as a "π-pulse". If the atom is initially in the ground state, then a π-pulse transfers it to the excited state. If the duration of the pulse is halved $T = \pi/(2\Omega)$ then, we obtain a "$\pi/2$-pulse", which transfers atoms initially in the ground state into an equal linear superposition of the ground and excited state. These pulses are very important in *Ramsey spectroscopy*, which is used in atomic clocks, and in quantum information processing where these types of pulses are examples of *single qubit operations*.

[1]Be careful however, as away from the context of CW optical spectroscopy the RWA is frequently violated. A good example is in the RF dressing of magnetic potentials to make novel atom traps.

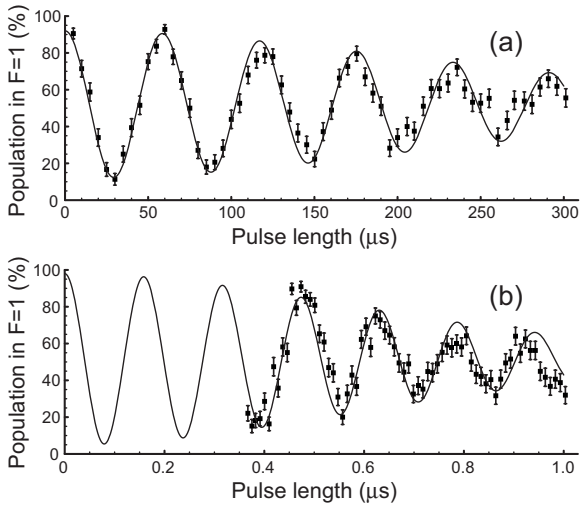

Figure 2: Rabi oscillations measured using a single ^{87}Rb atom trapped in an optical dipole trap. The $F = 1, m_F = 0 \rightarrow F = 2, m_F = 2$ transition at 6.8 GHz is driven using a two-photon Raman transition. In (a) the Rabi frequency is $\Omega = 2\pi \times 18$ KHz and in (b) it is $\Omega = 2\pi \times 6.7$ MHz. The damping is due to the finite temperature of the atoms in the trap. From [1]

1.1.2 AC Stark shifts

We can reformulate equations 8 and 9 to remove the explicit time dependence on the right hand side. Let us define new coefficients $c'_g = c_g$ and $c'_e = c_e e^{i\Delta t}$. In terms of these new coefficients, the equations of motion become

$$i\hbar \frac{dc'_g}{dt} = c'_e \frac{\hbar\Omega}{2} \tag{13}$$

$$i\hbar \frac{dc'_e}{dt} = c'_g \frac{\hbar\Omega}{2} - c'_e \hbar\Delta. \tag{14}$$

and the Hamiltonian can be written as[2]

$$\hat{H} = \frac{\hbar}{2} \begin{bmatrix} 0 & \Omega \\ \Omega & -2\Delta \end{bmatrix}. \tag{15}$$

We can diagonalise this Hamiltonian to find the eigenvalues and eigenvectors. The eigenvalues are

$$E_e = \frac{\hbar}{2}\left(-\Delta - \sqrt{\Omega^2 + \Delta^2}\right) \quad ; \quad E_g = \frac{\hbar}{2}\left(-\Delta + \sqrt{\Omega^2 + \Delta^2}\right) \tag{16}$$

Far from resonance where $\Omega \ll |\Delta|$ we can expand the square root, and we find that each state experiences a shift $\Delta E = \frac{\hbar\Omega^2}{4\Delta}$ that is proportional to the light intensity. The shift of the ground and excited states have opposite sign, and the overall sign depends on the sign of the detuning Δ. This shift is known as the *AC Stark shift* or the *lightshift*, and is exploited in optical dipole traps for cold atoms.

The new eigenvectors can be written as

$$|e'\rangle = \cos\theta|g\rangle - \sin\theta|e\rangle \quad ; \quad |g'\rangle = \sin\theta|g\rangle + \cos\theta|e\rangle \tag{17}$$

where $\cos 2\theta = -\Delta/\Omega'$. These states are known as the *dressed states*; the bare atom has been "dressed" by the off-resonant laser field. Each dressed state is a coherent superposition of the two bare eigenstates $|g\rangle$ and $|e\rangle$.

[2]Here we have chosen to write the Hamiltonian matrix as if it operated on a vector $\{c_g, c_e\}$ (i.e. the element in the top-left corner is the energy of the ground state). In this convention, we must identify state $|e\rangle$ with spin *down* and $|g\rangle$ with spin *up* if we are to use the conventional form of the Pauli spin matrices. In other words, the ground state $|g\rangle$ appears at the *top* of the Bloch sphere. This convention is used by *Loudon*, but the opposite is used in *Cohen-Tannoudji, Dupont-Roc and Gryndberg, "Atom-photon interactions"*. Of course both conventions yield the same optical Bloch equations.

2 Spontaneous emission and the density matrix

In the Schrödinger picture that we have considered thus far, the application of the classical light field causes the atom to oscillate between the ground and excited states. If we think in terms of energy transfer, then the conservation of energy implies that energy must be transferred to and from the monochromatic external light field. The processes that exchange energy with the driving field are known as *absorption* and *stimulated emission*. In this picture, an atom prepared in the excited state at $t = 0$ remains in the excited state, unless the external field is present to drive the atom.

In reality of course, atomic excited states have finite lifetimes. They decay by *spontaneous emission* - the emission of a photon into the empty modes of the electric field surrounding the atom. To describe atom-light interactions properly, we must include this process. Formally, we would need to write a Hamiltonian for our system that includes not only the coupling to the classical external driving field, but also to all the other electric field modes. To attack the problem in this way requires the techniques of quantum optics, which are beyond the scope of this course.

Instead we consider our atom as an isolated two level atom that is coupled to an environment (all the rest of the electric field). We don't care about the state of the environment, only about the state of our atom. The coupling between the atom and the environment is *irreversible* - when the atom spontaneously emits a photon it is "lost". The appearance of this irreversibility is an unavoidable consequence of our partial knowledge of the overall quantum state of the system+environment. The evolution described by the Schrödinger equation is symmetric in time, so we must look beyond this if we are to make progress.

2.1 The density matrix

2.1.1 Pure states and mixed states

Consider a beam of atoms prepared in an equal superposition state, for example by a $\pi/2$ pulse. The state of each atom can be completely described by the wavefunction

$$|\Psi\rangle = \frac{1}{\sqrt{2}}\left(|g\rangle + |e\rangle\right), \tag{18}$$

and the state of the N atoms in the beam can be described as a product of these wavefunctions:

$$|\Psi_{beam}\rangle = \left(|\Psi\rangle\right)^N. \tag{19}$$

This state, where it makes sense to talk about a wavefunction, is called a *pure state* [2].

Each atom in the beam passes through a device[3] that gives a click if the atom is in $|e\rangle$ and no click if it is in $|g\rangle$. What is the outcome of the measurement? if the atoms are in an equal superposition, we expect a click 50% of the time on average, with the clicks randomly distributed in time. Now consider the state of the atoms (and the beam) *after* the measurement. The measurement projects each atom in the beam into one of the two states so

$$|\Psi\rangle = |g\rangle \qquad OR \quad |\Psi\rangle = |e\rangle. \tag{20}$$

The beam therefore consists of a stream of atoms that are randomly in one state or the other, with equal probability. The beam is in a *statistical mixture* of the two states. This state cannot be described by the wavefunction Ψ_{beam}; in fact it cannot be described by a wavefunction at all. This type of state is called a *mixed state*. Note that this *mixed state* would still give a click 50% of the time on average if we were to repeat the measurement further downstream. How do we distinguish therefore between the state Ψ_{beam} and this statistical mixture? How can we represent them both in the same formalism? The answer is the *density matrix*

[3]For example, we could couple one of the states (but not the other) to a strong optical transition, and measure the fluorescence. Using this technique, ion trap experiments can make projective measurements on individual ions with $> 99.9\%$ fidelity [3]

2.1.2 The density matrix for for pure states

The *density operator for a state* is

$$\hat{\rho} = |\Psi\rangle\langle\Psi| \tag{21}$$

which is more conveniently written as a matrix - the *density matrix*, which for our two-level atom is

$$\hat{\rho} = \begin{pmatrix} \rho_{gg} & \rho_{ge} \\ \rho_{eg} & \rho_{ee} \end{pmatrix} = \begin{pmatrix} c_g c_g^* & c_g c_e^* \\ c_e c_g^* & c_e c_e^* \end{pmatrix}. \tag{22}$$

Asterisks (*) denote the complex conjugate. Each element is the product of two probability amplitudes. The diagonal matrix elements are the *square* of a probability amplitude, and are therefore straightforward to interpret as the *probability* of finding an atom in a particular state. The off-diagonal matrix elements are called it coherences. To see why this is the case let us consider the expectation value of an operator $\hat{A}$ acting on a state $\Psi\rangle = c_g|g\rangle + c_e|e\rangle$. One obtains $\langle A\rangle = |c_g|^2 A_{gg} + |c_e|^2 A_{ee} + 2\mathrm{Re}(c_g^* c_g A_{eg})$. The coherences describe the visibility of the interference, or cross-term, which depends on the relative phase between the states $|g\rangle$ and $|e\rangle$.

The density matrix for the pure state we considered above is $\hat{\rho} = \begin{pmatrix} 1/2 & i/2 \\ -i/2 & 1/2 \end{pmatrix}$. The coherences are not zero, and indeed if we applied a second $\pi/2$ pulse we can observe interference fringes in the probability to be in each of the two states.

2.1.3 The density matrix of mixed states

The huge advantage of the density matrix is that it can also describe mixed states. The density matrix for a mixed state is defined as

$$\hat{\rho} = \sum_i w_i |\Psi_i\rangle\langle\Psi_i|, \tag{23}$$

where w_i is the classical probability of being in state i. The density matrix is always diagonal for a completely mixed state. The density matrix for our atoms *after* the measurement is $\begin{pmatrix} 1/2 & 0 \\ 0 & 1/2 \end{pmatrix}$. The coherences have vanished. The coherences have vanished, and I would see no fringes on applying a second $\pi/2$ pulse.

2.2 The time evolution of the density matrix and spontaneous emission

If the evolution can be described in terms of of a Hamiltonian, then it can be easily shown that the time evolution of the density matrix is governed by the following equation:

$$\frac{d\rho}{dt} = \frac{i}{\hbar}\left[\hat{\rho}, \hat{H}\right] \tag{24}$$

where the term in square brackets is the commutator of the density operator and the Hamiltonian. This equation is called **Liouville's equation**; and it is equivalent to the Schrödinger equation.

However, the density matrix formalism also allows us to include processes which *can't* be described using a Hamiltonian, which allows us to include the effects of spontaneous emission. If the excited state $|e\rangle$ decays at rate Γ, then the time evolution of the populations due to spontaneous emission is

$$\frac{d\rho_{ee}}{dt} = -\frac{d\rho_{gg}}{dt} = -\Gamma\rho_{ee}. \tag{25}$$

The effect of spontaneous emission on the coherences is less obvious; here will just quote the result and refer to the literature for justification.

$$\frac{d\rho_{eg}}{dt} = -\frac{\Gamma}{2}\rho_{eg} \quad , \quad -\frac{d\rho_{ge}}{dt} = \frac{\Gamma}{2}\rho_{ge} \tag{26}$$

The full equation of motion for the density matrix, including the Hamiltonian part due to the interaction with the external field and spontaneous emission is

$$\frac{d\rho}{dt} = \frac{i}{\hbar}\left[\hat{\rho}, \hat{H}\right] - \begin{pmatrix} -\Gamma\rho_{ee} & \frac{\Gamma}{2}\rho_{ge} \\ \frac{\Gamma}{2}\rho_{eg} & \Gamma\rho_{ee} \end{pmatrix}. \tag{27}$$

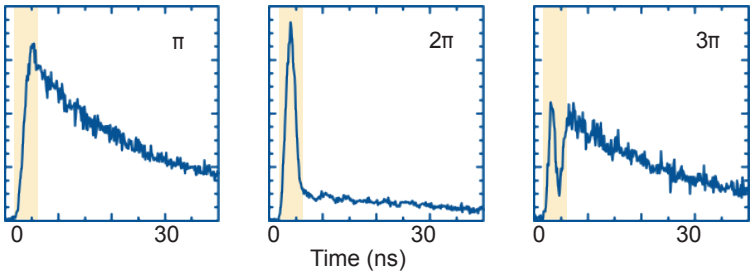

Figure 3: This figure illustrates the effects of coherent evolution and spontaneous emission. A single atom held in a dipole trap was illuminated by a 4 ns laser pulse (shaded region), and then left to evolve. Fluorescence photons emitted by the atom were collected by a lens and detected with high timing resolution. The amount of fluorescence depends on the population of the excited state. During the pulse, the laser drives Rabi oscillations between the ground and excited state. At the end of the laser pulse, the excited state population decays with the 27 ns lifetime of the excited state. From [4]

.

The most useful references for this section of the course are Ch. 5 of *Atom-photon interactions* by Cohen-Tannoudji *et al.* and Ch 2. of *The Quantum Theory of Light* by Loudon.

3 The optical Bloch equations

At the end of the previous section we wrote down the following matrix equation for the evolution of the density matrix:

$$\frac{d\rho}{dt} = \frac{i}{\hbar}\left[\hat{\rho}, \hat{H}\right] - \begin{pmatrix} -\Gamma\rho_{ee} & \frac{\Gamma}{2}\rho_{ge} \\ \frac{\Gamma}{2}\rho_{eg} & \Gamma\rho_{ee} \end{pmatrix}. \tag{28}$$

Using the time-independent form of the Hamiltonian that we introduced in the previous section

$$\hat{H} = \frac{\hbar}{2}\begin{bmatrix} 0 & \Omega \\ \Omega & -2\Delta \end{bmatrix}, \tag{29}$$

we can expand the commutator and write out this matrix equation as a system of coupled differential equations

$$\dot{\tilde{\rho}}_{gg} = \frac{i\Omega}{2}\left(\tilde{\rho}_{ge} - \tilde{\rho}_{eg}\right) + \Gamma\tilde{\rho}_{ee} \tag{30}$$

$$\dot{\tilde{\rho}}_{ee} = -\frac{i\Omega}{2}\left(\tilde{\rho}_{ge} - \tilde{\rho}_{eg}\right) - \Gamma\tilde{\rho}_{ee} \tag{31}$$

$$\dot{\tilde{\rho}}_{ge} = -\frac{i\Omega}{2}\left(\tilde{\rho}_{ee} - \tilde{\rho}_{gg}\right) - i\Delta\tilde{\rho}_{ge} - \frac{\Gamma}{2}\tilde{\rho}_{ge} \tag{32}$$

$$\dot{\tilde{\rho}}_{eg} = \frac{i\Omega}{2}\left(\tilde{\rho}_{ee} - \tilde{\rho}_{gg}\right) + i\Delta\tilde{\rho}_{eg} - \frac{\Gamma}{2}\tilde{\rho}_{eg} \tag{33}$$

These equations[4] are known as the **optical Bloch equations.**. Their solutions have been studied extensively; analytical solutions are possible in only a few special cases, but the equations can be solved numerically by standard techniques. In addition to these equations, the elements of the density matrix must obey two other constraints: the sum of the populations $\tilde{\rho}_{gg} + \tilde{\rho}_{ee} = 1$, and the off-diagonal matrix elements are complex conjugates ($\tilde{\rho}_{ge} = \tilde{\rho}^*_{eg}$). In fact, only three independent components need be considered, which we can write as the components $\{u, v, w\}$ of a vector known as the **Bloch vector**, where

$$u = \frac{1}{2}\left(\tilde{\rho}_{ge} + \tilde{\rho}_{eg}\right) \qquad v = \frac{1}{2i}\left(\tilde{\rho}_{eg} - \tilde{\rho}_{ge}\right) \qquad w = \frac{1}{2}\left(\tilde{\rho}_{gg} - \tilde{\rho}_{ee}\right). \tag{34}$$

[4]Here the tilde is used to denote the fact that we have used the time-independent form of the Hamiltonian. Bear in mind also that we have made the rotating wave approximation

We can attach a physical significance to each of the three terms: w is proportional to the difference in the populations of the ground and excited state, and u and v are respectively proportional to the in phase and quadrature components of the atomic dipole moment, as we will show later. The differential equations describing the evolution of the Bloch vector are easily derived from equations 30. The Bloch vector has a maximum of unit length, and in the absence of spontaneous emission this unit vector defines a point on the *Bloch sphere* as shown in Fig. 4. The effect of spontaneous emission is to "collapse" the Bloch sphere; the Bloch vector no longer has unit length and the sphere eventually shrinks to a single point as all the atoms end up in the ground state.

3.1 The steady-state solution

By setting the time derivatives to zero, we obtain the steady-state solutions for constant Ω. They can be written as:

$$u_{ss} = \frac{\Delta}{\Omega}\frac{S}{1+S} \qquad v_{ss} = \frac{\Gamma}{2\Omega}\frac{S}{1+S} \qquad w_{ss} = \frac{1}{2}\left(\frac{S}{1+S} - 1\right) \tag{35}$$

where we have introduced the saturation parameter S

$$S = \frac{\Omega^2/2}{\Delta^2 + (\Gamma^2/4)} = \frac{s}{1 + 4\Delta^2/\Gamma^2}, \tag{36}$$

where the on-resonant saturation parameter $s = I/I_{\rm sat}$. The saturation intensity $I_{\rm sat}$ is a commonly used way of describing the strength of a transition, as it is conveniently related to things that can be measured in the lab. It can be written as

$$I_{\rm sat} = \frac{2\pi^2\hbar\Gamma c}{3\lambda^3} \tag{37}$$

and can be thought of as an energy (photon energy hc/λ) per unit time (lifetime $1/\Gamma$) per unit area (the resonant cross-section is approximately λ^2). For D lines of the alkali metals, $I_{\rm sat} \approx 1$ mW cm^{-2}.

3.2 Properties of the steady-state solution

The steady-state population of the excited state is

$$\tilde{\rho}_{ee} = w_{ss} + 1/2 = \frac{1}{2}\frac{s}{1 + s + 4\Delta^2/\Gamma^2}. \tag{38}$$

Let us compare this solution with the Rabi solution that we discussed previously. There, the application of a constant driving field led to Rabi oscillations, and on resonance, the population could be transferred completely from the ground state to the excited state and back. In the presence of damping, oscillations are no longer observed[5]. Instead the population reaches a steady state given by equation 38. The maximum population of the excited state is $\tilde{\rho}_{ee} = 1/2$, which is attained only asymptotically as the laser intensity is increased. This effect is known as *saturation*[6].

From equation 38, we can calculate the scattering rate R

$$R(I, \Delta) = \Gamma\tilde{\rho}_{ee} = \frac{\Gamma}{2}\frac{s}{1 + s + 4\Delta^2/\Gamma^2}. \tag{39}$$

This expression for the scattering rate is one of the key results of the Bloch equation treatment. As an example, consider the measurement of the number of atoms N in a cloud of laser-cooled atoms. Applying a resonant probe beam causes the atoms to fluoresce, and we can collect the fluorescence and image it onto a photodiode. If the total collection efficiency of our detection system (including the sold angle and the photodiode calibration is ϵ, then the photodiode signal $S_{\rm PD} = RN/\epsilon$.

The scattering rate has a Lorentzian lineshape, with width $\Gamma' = \sqrt{\Gamma^2(1+s)}$ At low intensity ($s \ll 1$), the width is set by the *natural linewidth* Γ. At higher intensity, the width increases and the line becomes *power broadened*.

[5] In the homework you will show that coherent dynamics can only be observed on timescales that are short compared to Γ. See also the graphs of Rabi oscillations followed by spontaneous decay in the previous section.

[6] It is important to note that saturation arises because the system is *closed*; the only decay mechanism transfers population back to the ground state. In the case of solid state systems or molecules, there may be no closed transitions, and decay may occur to many different states. In this case, saturation may not occur

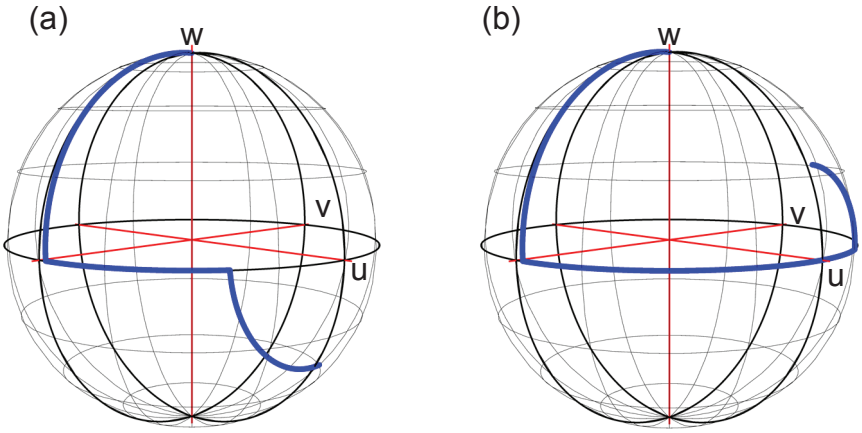

Figure 4: The three components of the Bloch vector can be used to define a point in a three-dimensional space {u,v,w}. In the absence of spontaneous emission, these points are constrained to lie on a sphere, called the *Bloch sphere*. By numerically solving the optical Bloch equations, we can plot the evolution of the system as a trajectory on the Bloch sphere. In this case, (a) and (b) both show trajectories for a double $\pi/2$-pulse Ramsey-type experiment. The first $\pi/2$ pulse rotates the Bloch vector into the equatorial plane, corresponding to an equal superposition of the ground and excited state. A period of free evolution follows. As there is a finite detuning Δ, the Bloch vector rotates in the equatorial plane. Depending on the length of the free evolution, the second $\pi/2$ pulse transfers a varying amount of the population to the excited state

3.3 Time-dependent solutions

The optical Bloch equations can be solved numerically in the case of a time-dependent driving field. Figure 4 shows the numerical solution for the three components of the Bloch vector for a Ramsey type experiment, where two $\pi/2$ pulses are separated by a period of free evolution. You will investigate some time-dependent solutions in one of the homeworks.

4 Relating the microscopic and macroscopic

The optical Bloch equations allow us to calculate the state of a single two-level atom interacting with a classical light field. In this section we will investigate how we can relate this microscopic theory for a single atom to the observations such as absorption spectra that we make in the lab. We will start by looking at the macroscopic theory of dielectrics[7], which will lead us to introduce the susceptibility as the key parameter that describes the absorptive and dispersive properties of the medium. By relating the susceptibility to the dipole moment of a single atom, we will make the connection between the macroscopic properties of the medium and the theory for single atoms that we have developed so far.

4.1 The susceptibility

The response of a dielectric (in this case an ensemble of two-level atoms) to an external electric field $\vec{E}$ can be written as

$$\vec{P} = \epsilon_0 \chi(\omega) \vec{E}. \tag{40}$$

The constant of proportionality $\chi(\omega)$ is called the *susceptibility* of the medium, and the factor of ϵ_0 ensures that χ is dimensionless. Here we have assumed that the electric polarization $\vec{P}$ (dipole moment per unit volume), is proportional to the applied field - in other words that we are dealing with *linear* optics. For intense fields the polarization can depend on higher orders of the electric field, giving rise to the domain of nonlinear optics[8].

[7] If you are not familiar with this, then a good reference is *Classical Electrodynamics* by Jackson.

[8] We have also assumed that the medium is isotropic, such that the induced field is parallel to the applied field. In crystals this is not always the case, and the susceptibility becomes a tensor. We have also assumed that the medium

The susceptibility is frequency dependent, and it is *complex*; the *real* part describes the dispersive properties and the *imaginary* part describes the absorption. Inside the medium, Maxwell's equations must be rewritten in terms of the electric displacement vector $\vec{D} = \epsilon_0\vec{E} + \vec{P} = \epsilon 0\vec{E} + \epsilon 0\chi\vec{E} = \epsilon_r\epsilon_0\vec{E}$, where the dielectric constant, or relative permittivity, is $\epsilon_r = 1+\chi$. Plane wave solutions propagate at a modified speed $v = 1\sqrt{\epsilon_r\mu_r}$, and we are led to introduce the refractive index $n = \sqrt{\epsilon_r\mu_r} = \sqrt{\epsilon_r}$, where we have used the fact that the magnetic response of the medium is negligible at optical frequencies (this essentially the same as the electric dipole approximation). Now, the refractive index modifies the propagation of a plane wave in the following way: $\vec{E} = \vec{E}_0 e^{i(kz-\omega t)} \rightarrow \vec{E} = \vec{E}_0 e^{i(nkz-\omega t)}$. A natural extension is to allow the refractive index to be complex, i.e. $n = n_\mathrm{R} + in_\mathrm{I}$. In this case, we obtain $\vec{E} = \vec{E}_0 e^{i(kz-\omega t)} \rightarrow \vec{E} = \vec{E}_0 e^{i(n_\mathrm{R}kz-\omega t)} e^{-(kn_\mathrm{I}z)}$. The imaginary part leads to an exponentially decaying amplitude and therefore describes *absorption*. We can relate the imaginary and real parts of χ to the corresponding parts of the refractive index as follows:

$$n = \sqrt{1+\chi} \approx 1 + \frac{\chi}{2} \tag{41}$$

$$\therefore n_\mathrm{R} = 1 + \frac{\chi_\mathrm{R}}{2}; \quad n_i = \frac{\chi_\mathrm{I}}{2} \tag{42}$$

Thus, if we can calculate the susceptibility, then the absorptive and dispersive properties of the medium follow.

Before we examine the calculation of the susceptibility, we note that the dispersive and absorptive properties are inextricably linked. They are related by the **Kramers-Kronig** relations,

$$\chi_\mathrm{R}(\omega) = \frac{2}{\pi}\int_0^\infty \frac{\omega'\chi_\mathrm{I}(\omega')}{w'^2-\omega^2}d\omega' \tag{43}$$

$$\chi_\mathrm{I}(\omega) = -\frac{2\omega}{\pi}\int_0^\infty \frac{\chi_\mathrm{R}(\omega')}{w'^2-\omega^2}d\omega', \tag{44}$$

which can be derived from fundamental considerations of the theory of complex functions and the principle of causality. As such they hold generally, and in particular they are independent of any model (linear or nonlinear) for χ.

4.2 The dipole moment of a single atom

The approach that we take to calculating the susceptibility is to first calculate the polarisation $\vec{P}$ from the dipole moment of a single atom, and then use equation 40 to obtain an expression for the susceptibility. The dipole moment of a single atom can be calculated from the optical Bloch equations. To do this we make use of the general result that the expectation value of *any* operator $\hat{A}$ is given by $\langle A\rangle = \mathrm{Tr}(\hat{\rho}\hat{A})$.

As we have already seen, the dipole operator can be written as $\hat{d} = \begin{pmatrix} 0 & d_{ge} \\ d_{eg} & 0 \end{pmatrix}$ where $d_{ge} = \langle g|\hat{d}\cdot\hat{\epsilon}|e\rangle E_0$. Therefore we find

$$\langle d\rangle = \mathrm{Tr}(\hat{\rho}\hat{d}) = d_{ge}(\rho_{ge}+\rho_{ge}) \tag{45}$$

$$= d_{ge}(\tilde{\rho}_{ge}e^{-i\omega t} + \tilde{\rho}_{eg}e^{i\omega t}) \tag{46}$$

$$= 2d_{ge}(u\cos\omega t - v\sin\omega t). \tag{47}$$

We can now identify u and v as respectively proportional to the components of the atomic dipole in phase and in quadrature with the incident field. Re-writing equation 40 as $\vec{P} = \frac{1}{2}\epsilon_0\vec{E}(\chi e^{-i\omega t} + \chi^* e^{i\omega t})$ we have

responds instantaneously, and that there are no ferroelectric effects (permanent dipole moment).

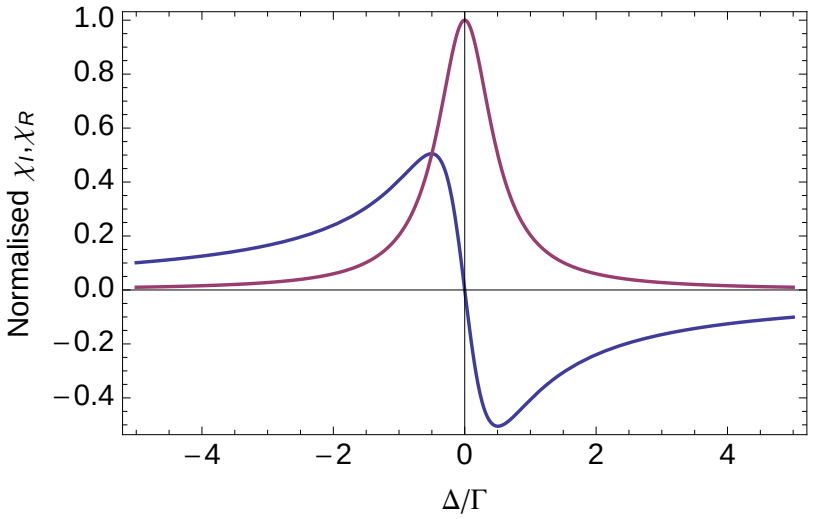

Figure 5: Normalised absorption $\chi_{\mathrm{I}}(\Delta)/\chi_{\mathrm{I}}(0)$ (red) and dispersion $\chi_{\mathrm{R}}(\Delta)/\chi_{\mathrm{I}}(0)$ (blue) as a function of detuning Δ, with $\Gamma = 1$ and $\Omega = 0.1$.

$$\vec{P} = n\langle\hat{d}\rangle = \frac{1}{2}\epsilon_0\vec{E}(\chi e^{-i\omega t} + \chi^* e^{i\omega t}) \tag{48}$$

$$nd_{ge}(\tilde{\rho}_{ge}e^{-i\omega_L t} + \tilde{\rho}_{eg}e^{i\omega_L t}) = \frac{1}{2}\epsilon_0\vec{E}(\chi e^{-i\omega t} + \chi^* e^{i\omega t}) \tag{49}$$

$$\therefore \chi = \frac{-2nd_{ge}}{\epsilon_0}\tilde{\rho}_{ge}, \tag{50}$$

where $n = N/V$ is the atomic number density. An important point to note is that the atomic dipole and are related to the *off-diagonal* matrix elements $\tilde{\rho}_{ge,eg}$ of the density matrix. This result can be generalised in a relatively straightforward way to obtain the susceptibility in cases involving more than two levels [5].

4.3 The susceptibility of a two-level atom

The steady-state susceptibility can be found by noting that$\tilde{\rho}_{ge} = u - iv$, and substituting equations 35 into equation 48[9] . Splitting the result into real and imaginary parts, one finds:

$$\chi_{\mathrm{R}} = \frac{2nd_{ge}}{\epsilon_0}u = -\frac{nd_{ge}^2}{\hbar\epsilon_0}\frac{\Delta}{\Delta^2 + \Gamma^2/4 + \Omega^2/2} \tag{51}$$

$$\chi_{\mathrm{I}} = -\frac{2nd_{ge}}{\epsilon_0}v = \frac{nd_{ge}^2}{\hbar\epsilon_0}\frac{\Gamma/2}{\Delta^2 + \Gamma^2/4 + \Omega^2/2} \tag{52}$$

where we have used $\hbar\Omega = -d_{ge}$. The real and imaginary parts of the steady-state susceptibility are plotted as a function of detuning in Fig. 5. The absorption has a familiar Lorentzian lineshape. The dispersion however is quite different: it is an odd function, which changes sign exactly on resonance. The dispersion is positive below resonance, and negative above resonance. The shape of this curve is known as a "dispersion lineshape" and it is intimately related to the Lorentzian lineshape of the absorption via the Kramers-Kronig relations.

4.4 Saturated absorption

In our discussion of susceptibility, we wrote that the electric field after propagating a distance z through the atomic vapour is $\vec{E} = \vec{E}_0 e^{i(n_{\mathrm{R}}kz - \omega t)}e^{-(kn_{\mathrm{I}}z)}$. The intensity $I = I_0 e^{-\alpha z}$, where α is known

[9]In other words, the real part of χ (dispersion) arises from the component of the atomic dipole that is *in phase* with the driving field, and the imaginary part (absorption) arises from the *quadrature* component.

as the absorption coefficient. Using the relation $I = \frac{1}{2}\epsilon_0 c E^2$ we can identify that

$$\alpha = 2kn_{\mathrm{I}} \tag{53}$$
$$= k\chi_{\mathrm{I}}. \tag{54}$$

The amount of light absorbed by a slab of atoms of thickness $dz = \alpha dz$, and so the transmission through the medium is governed by the differential equation

$$\frac{1}{I}\frac{dI}{dz} = -k\chi_{\mathrm{I}} \tag{55}$$
$$\Rightarrow \frac{dI}{dz} = -I\frac{knd_{ge}^2}{\hbar\epsilon_0}\frac{\Gamma/2}{\Delta^2 + \Gamma^2/4 + \Omega^2/2} \tag{56}$$

Re-writing this in terms of the on-resonant saturation parameter s we obtain

$$\frac{dI}{dz} = -n\hbar\omega\frac{\Gamma}{2}\frac{s}{1 + s + 4\Delta^2/\Gamma^2}. \tag{57}$$

The absorption coefficient α is intensity dependent - despite considering a linear model for the susceptibility at the beginning, we have ended up with a non-linear response of the medium. It is interesting to consider the extremes of low and high intensity. At low intensity $s \ll 1$ and equation 57 becomes

$$\frac{1}{I}\frac{dI}{dz} = -\frac{n\hbar\omega}{I_{\mathrm{sat}}}\frac{\Gamma}{2}\frac{1}{1 + 4\Delta^2/\Gamma^2}. \tag{58}$$

The solution of this equation yields the well-known *Beer Lambert law*: the intensity decays exponentially with distance propagated through the medium. In the high-intensity limit $s \gg 1$ and we have

$$\frac{dI}{dz} = -n\hbar\omega\frac{\Gamma}{2}. \tag{59}$$

The solution in this regime is $I = I_0 - zn\hbar\omega\Gamma/2$ - there is a *linear* decrease in absorption with distance propagated. It is straightforward to show that as the intensity increases, saturation causes the medium to transmit a significantly larger fraction of the incident intensity. In other words, the absorption becomes *saturated*. The physical origin of this effect becomes apparent if we note that we can derive equation 57 by considering the rate at which light is scattered out of the medium. The power scattered by a single atom is $\hbar\omega R = \hbar\omega\Gamma\rho_{ee}$, and by considering the power scattered out of the beam by a slab of density n and thickness dz one obtains equation 57[10]. As you have shown in the homework, the excited state population ρ_{ee} and hence the scattered power saturates at high intensity. As the medium cannot scatter any more light, the transmission increases. This principle underlies one of the most important forms of sub-Doppler spectroscopy, known as *saturated absorption spectroscopy*, which you will look at in the homework.

[10]Its often a good sign if energy in = energy out

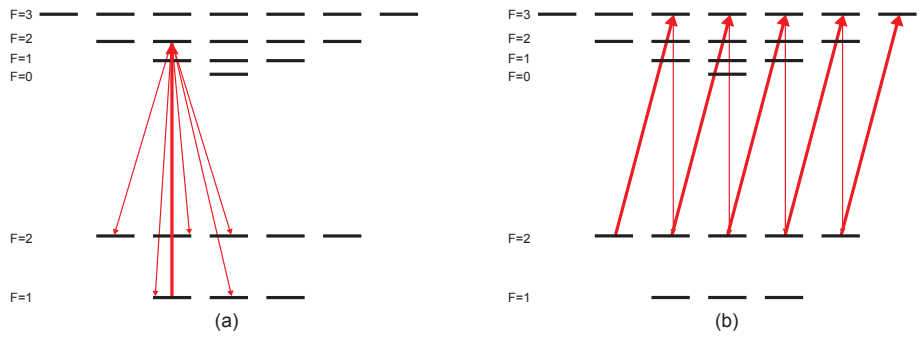

Figure 6: Examples of optical pumping in ^{87}Rb. (a) Hyperfine pumping. The transition $F = 1 \rightarrow F' = 2$ is clearly not closed, and driving this transition will pump population into the $F = 2$ ground state hyperfine level. (b) Zeeman pumping. It is also possible to pump atoms into an individual m_F state. here circularly polarised light pumps the atoms into the $F = 2, m_F = 2$ state. Note that only some of the spontaneous decay paths are shown for clarity.

5 Beyond two levels

In this section we will look at the effects of moving beyond the two-level atom approximation. In the first part we will consider optical pumping - an important *incoherent* effect that arises from the availability of more decay channels. In the second part we will consider some of the *coherent* effects that can arise when three levels and two laser fields are involved. These include electromagnetically induced transparency (EIT) and Raman transitions.

5.1 Optical Pumping

Let us consider once again our favourite transition - the D2 line in ^{87}Rb. The energy level diagram is shown in Fig. 6. Now imagine that i start with atoms that are all in the lowest energy level: the $F = 1$ hyperfine ground state. Note that there is only one possible closed transition from this level[11]. If we excite to the $F' = 2$ state, then this energy level can decay to the $F = 2$ sublevel in the ground state, as well as the original $F = 1$ sublevel. Crucially, once the atom is in $F = 2$, it is no longer resonant with the laser, and it will stay there. As a result, the population accumulates in $F = 2$. This is known as *optical pumping*; we say that the population has been *pumped* into the $F = 2$ state by the laser. As it relies on spontaneous emission, this transfer process is *incoherent* (it does not setup additional off-diagonal elements in the density matrix). The transfer can in principle be close to 100% efficient[12] - ALL the atoms can be transferred to $F = 2$. Therefore optical pumping is often used for state preparation. Optical pumping can also be a problem in some experiments. Laser cooling experiments in Rb use the $F = 2 \rightarrow F' = 3$ closed transition. However, off-resonant excitation of the other hyperfine levels is possible, and this leads to optical pumping into the $F = 1$ level, and an additional *repump* laser must be used to empty this state and return the atoms to the to the cooling cycle.

Optical pumping can also be used to prepare atoms in a particular m_F sublevel by controlling the light polarization. Consider a circularly polarised beam resonant with the $F = 2 \rightarrow F' = 3$ transition as shown in Fig. 6(b). The quantization axis is defined by a magnetic field applied along the propagation direction of the beam, such that it drives σ^+ transitions with $\Delta m_F = +1$. A sequence of absorption and spontaneous emission cycles will pump the atom into the "stretched state" $|F = 2, m_F = +2\rangle$, where it will cycle on the completely closed $F = 2, m_F = 2 \rightarrow F' = 3, m_F = 3$ transition. Other optical pumping schemes are possible where the final state is a "dark state" which is no longer coupled to the laser beams, which have the advantage that once pumped, the atoms are not heated by spontaneous emission.

[11] which one?
[12] what effects might prevent 100% transfer?

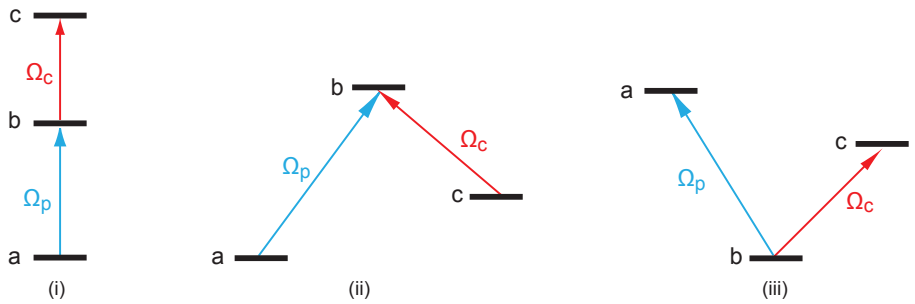

Figure 7: The three possible arrangements of three levels and two fields: (i) "ladder" or "cascade" (ii) "lambda" (iii) "vee".

5.2 The three-level system

To look at coherent effects in multi-level atoms, we will add one more level and one more laser field to the two-level atom that we have discussed so far. It is possible to derive optical Bloch equations for this three-level system, which you will look at in the homework, and which provide a unified theoretical framework. Here we will discuss in more general terms the physical effects that can be observed in this system. Two very useful articles on this subject are [5] and [6].

There are three distinct ways that the three levels and two laser fields can be arranged, as shown in Fig 7. In this section we will consider the "lambda" and "cascade" systems, as it is difficult to see coherent effects on the "vee" system.

5.3 Dressed states revisited - Autler-Townes splitting

Consider a cascade or ladder system of levels. The lower two levels $|a\rangle$ and $|b\rangle$ form a closed two-level system identical to that which we have studied previously. In the dressed state picture, coupling these two-levels with a strong resonant probe laser field Ω_p leads to two new eigenstates, which are separated by $\pm\Omega_p/2$. Now let us add a weak coupling laser which probes the transition from $|b\rangle$ to $|c\rangle$. As state $|b\rangle$ is present in both dressed states, they are *both* coupled to $|c\rangle$ by the laser. If we measure the population in $|c\rangle$, for example by using fluorescence, then we will observe a *doublet* of spectral lines, where the splitting is governed by the probe Rabi frequency Ω_p, as shown in Fig 8. This is called the *Autler-Townes* splitting.

5.4 Interference in the dressed state picture - CPT and EIT

Keeping this picture of dressed states in mind, let us turn to the "lambda" scheme. Let the states $|b\rangle$ and $|c\rangle$ be coupled by a strong laser field Ω_c. As in the previous example, a weak probe beam on the $|a\rangle$ to $|b\rangle$ transition interacts with the dressed states of the coupled system. There are two possible excitation pathways from $|a\rangle$ to $|b\rangle$, via each of the two dressed states. If the probe beam is exactly on resonance, then the probability amplitudes for each of these pathways are equal and opposite, and they can *cancel*. In other words, instead of the probe beam being strongly absorbed exactly on resonance, it is transmitted. the medium has become at least partially transparent to the probe beam; this effect is commonly known as *electromagnetically induced transparency*.

To understand this in a little more detail, it is useful to look at the dressed states of the three-level system. We will follow (with a slight change in notation) the treatment presented in [6]. The Hamiltonian can be written as[13]

$$\hat{H} = \frac{\hbar}{2}\begin{pmatrix} 0 & \Omega_p & 0 \\ \Omega_p & -2\Delta_p & \Omega_c \\ 0 & \Omega_c & -2(\Delta_p - \Delta_c) \end{pmatrix} \tag{60}$$

where Δ_p and Δ_c are respectively the detuning of the probe and coupling lasers. The form of this Hamiltonian is simple to understand; the four elements in the top left corner refer to the probe

[13]This Hamiltonian is written for the "slow variables" i.e. we have transformed out terms like $e^{i\omega t}$.

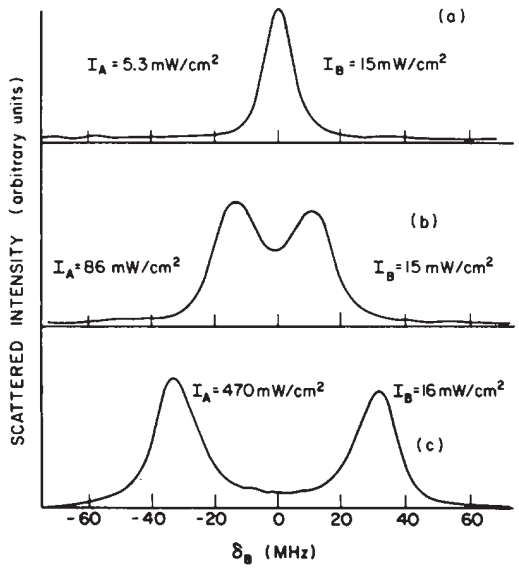

Figure 8: Autler-Townes doublet observed in ladder system using a beam of Na atoms. The probe laser (A) is tuned exactly on resonance, and the coupling laser (B) is scanned across the $|b\rangle \rightarrow |c\rangle$ transition. The splitting increases as the probe laser frequency is increased. Figure from [7].

transition and are identical to the Hamiltonian we obtained for the two level atom. All we have done in the remainder of the matrix, is to add the coupling of levels $|b\rangle$ and $|c\rangle$, and the (relative) energy of state $|c\rangle$.

The eigenstates of this Hamiltonian can be expressed in terms of mixing angles. For two-photon resonance ($\Delta_c = \Delta_p = \Delta$) the mixing angles can be written as

$$\tan\theta = \frac{\Omega_p}{\Omega_c} \tag{61}$$

$$\tan 2\phi = \frac{\sqrt{\Omega_p^2 + \Omega_c^2}}{\Delta} \tag{62}$$

and the three eigenstates are:

$$|\psi_+\rangle = \sin\theta\sin\phi|a\rangle + \cos\phi|b\rangle + \cos\theta\sin\phi|c\rangle \tag{63}$$

$$|\psi_0\rangle = \cos\theta|a\rangle - \sin\theta|c\rangle \tag{64}$$

$$|\psi_-\rangle = \sin\theta\cos\phi|a\rangle - \sin\phi|b\rangle + \cos\theta\cos\phi|c\rangle. \tag{65}$$

The two states Ψ_+ and Ψ_- contain a component of the excited state $|b\rangle$, whereas the state Ψ_0 does not. If an atom is prepared in Ψ_0 there is no possibility of excitation to $|b\rangle$ and subsequent spontaneous emission:- it is a *dark state*. In contrast Ψ_+ and Ψ_- do give rise to fluorescence; they are the dressed states responsible for the Autler-Townes doublet described above.

How much each of the three eigenstates is populated depends on the evolution of the system. For example, the dark state can be populated by optical pumping. In this case population steadily accumulates in the dark state where it is trapped - an effect known as *coherent population trapping*. Alternatively, the dark state can also be populated adiabatically. Consider a weak probe beam for which $\Omega_p \ll \Omega_c$, or $\theta \approx 0$. In this limit, the dark state ψ_0 becomes identical to the ground state $|0\rangle$, and excitation cannot occur. If Ω_p is increased sufficienty slowly, the population will remain in the dark state as θ and ϕ evolve. It is this effect that gives rise to electromagnetically induced transparency. Adiabatic evolution can also be exploited to transfer population efficiently from $|a\rangle$ to $|c\rangle$ without ever populating $|b\rangle$ in a technique known as *stimulated Raman adiabatic passage* or STIRAP [8].

A more complete description of all these effects (CPT, EIT and STIRAP) can be obtained by solving the optical Bloch equations for the three-level system, which we will investigate in the homework.

Before we move on to off-resonant effects, it is important to note that similar effects can be observed using a ladder scheme of energy levels. At first glance, this is not surprising given that it just involves a re-labelling of states in the Hamiltonian. However, in our discussion of the lambda scheme we have implicitly assumed that the state $|a\rangle$ and $|c\rangle$ are stable. This is not the case in a ladder scheme, where decay from $|c\rangle \to |b\rangle$ and from $|c\rangle \to |a\rangle$ becomes possible, and must be taken into account.

5.5 Raman transitions

So far, we have considered both lasers to be close to resonance with their respective optical transitions i.e. $\Delta_p = \Delta_c \approx 0$. Another important limit occurs when the one-photon detuning $\Delta = \Delta_p + \Delta_c$ is very large ($\Delta \gg \Omega_c, \Omega_p$), but the two-photon resonance condition ($\delta = \Delta_c - \Delta_p = 0$) is met. Some insight into this regime can be gained by looking at the dressed states in the limit of large Δ. We obtain

$$|\psi_+\rangle = |b\rangle \tag{66}$$

$$|\psi_0\rangle = \cos\theta|a\rangle - \sin\theta|c\rangle \tag{67}$$

$$|\psi_-\rangle = \sin\theta|a\rangle + \cos\theta|c\rangle. \tag{68}$$

As the lasers are far from one -photon resonance, the excited state $|b\rangle$ is not significantly populated. Levels $|a\rangle$ and $|b\rangle$ behave like an isolated two-level system with an effective Rabi frequency that depends on both the probe and coupling lasers. More rigourously, one can show [9] that the excited state $|b\rangle$ can be "adiabatically eliminated" from the optical Bloch equations, which reduce to the Bloch equations for a coherent two-level system with an effective Rabi frequency $\Omega' = \frac{\Omega_p \Omega_c}{\Delta}$. In other words, the lasers drive an off-resonant, two-photon transition between the states $|a\rangle$ and $|c\rangle$, which in this ideal limit does not populate $|b\rangle$ and lead to spontaneous emission. Note that as this is a two-photon transition, the usual electric dipole selection rules are modified. In particular, it is possible to drive Raman transitions between states with $\Delta L = 0$, which means that Raman transitions can be used to drive transitions between the hyperfine ground states of the alkalis. Raman transitions crop up throughout modern atomic physics, as they can be used to perform qubit operations, for cooling and for many other high-precision spectroscopy experiments. They are also important in condensed matter systems, where they are often used to couple light with phonons.

6 Basic atomic structure

This part of the graduate course is a revision of the origin of the basic structure of atomic energy levels. A detailed discussion is beyond the scope of these lectures; you are referred to *Woodgate* and *Bransden and Joachim* for more details.

6.1 Gross structure

The gross structure of atomic energy of hydrogen is of course obtained from the solution of the Schrödinger equation for a Coulomb potential. The resulting wavefunctions can be written as a product of a radial wavefunction that depends on two quantum numbers - the principal quantum number n and the orbital angular momentum l, and an angular wavefunction that depends on l and its projection m_l. At this level of approximation, all states of a given n are degenerate in l, and the energy levels are given by the Rydberg formula:

$$E_H = hc\frac{R}{n^2} \tag{69}$$

where R_{inf} is the Rydberg constant. For alkali atoms, a modified version of the same equation can be written:

$$E_{Rb} = hc\frac{R_{Rb}}{(n-\delta_l)^2} \tag{70}$$

where δ_l is known as the *quantum defect* which arises because the outer valence electron no longer experiences a pure Coulomb potential. The quantum defect is l dependent, breaking the degeneracy observed in hydrogen. This equation is a good description of the energy levels for Rydberg states where $n > 10$. The quantum defects determine many of the properties of Rydberg atoms, including their behaviour in external fields and their interactions [10].

6.2 Fine structure

The fine structure is a result of relativistic effects that are not described by the Schrödinger equation. The most important of these is the intrinsic angular momentum, or spin s, of the electron. The electron spin can couple to the orbital angular momentum of the electron via the *spin-orbit* interaction

$$\hat{H}_{FS} = \sum_i \xi_i \hat{l}_i \cdot \hat{s}_i \tag{71}$$

where ξ_i is a constant that depends on the radial wavefunction of the electron, and we sum over the i valence electrons (the sum over closed shells is zero). This leads naturally to the introduction of another quantum number: the total angular momentum of each electron j_i, and the eigenstates of the spin-orbit Hamiltonian are the eigenstates of the $\hat{j}_i = \hat{l}_i + \hat{s}_i$ (see problems). For a single valence electron, we do not need to worry about the summation. The fine structure splitting of Rb is illustrated in Fig. 9. The fine structure leads to a splitting of the 5P state, giving a *doublet* of spectral lines that are commonly labelled $D1$ and $D2$.

For two or more electrons, the situation is slightly more complicated, as one must compare the size of the fine structure splitting to other effects that occur due to the Coulomb interaction between the two electrons. This interaction also lifts the degeneracy of different spin states in a given *configuration* (e.g. 5s5p). In general this interaction is much larger than the fine-structure splitting. This situation is known as *L-S coupling*. In this case the residual Coulomb interaction splits the $5s5p$ configuration into two terms: ^1P and ^3P. Within each term, L and S remain good quantum numbers, and the fine structure Hamiltonian can be written as

$$\hat{H}_{FS} = A_{FS}\hat{L} \cdot \hat{S} \tag{72}$$

This leads to a splitting of the three different J states associated with ^3P term. We will look at the effect of the breakdown of L-S coupling in the homework

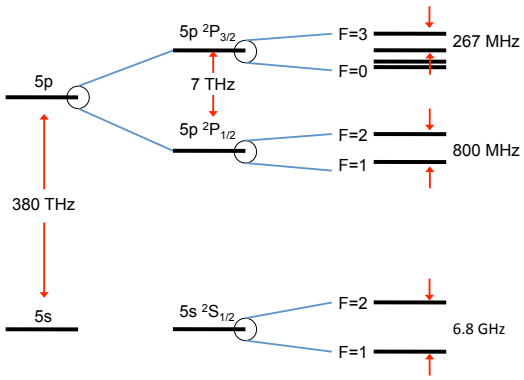

Figure 9: The hierarchy of energy scales illustrated for ^{87}Rb, showing how the levels split as we add the fine and hyperfine interactions. Detailed numbers for energies, splittings and wavelengths for Rb can be found in [11].

.

6.3 Hyperfine structure

Hyperfine structure is the result of the interaction between the electrons and the nucleus. The dominant effects that give rise to a splitting of the energy levels are the magnetic dipole interaction and the electric quadrupole interaction. We will discuss these further in the discussion of multipole expansions in the lecture notes, and in next weeks homework. Here as an example we will consider the hyperfine splitting of s states (e.g. Rb ground state) where the quadrupole term vanishes.

The magnetic dipole interaction is the interaction between the magnetic dipole μ_I associated with the nuclear spin I and the magnetic field produced by the orbiting electrons at the nucleus B_el

$$\hat{H}_{hfs} = -\hat{\mu} \cdot \hat{B}_e l. \tag{73}$$

As the hyperfine splitting is smaller than all electronic energy scales[14], this interaction takes the form of a coupling between the nuclear spin I and the total electronic angular momentum j

$$\hat{H}_{hfs} = A\hat{I} \cdot \hat{J}. \tag{74}$$

This is analogous to the LS coupling described above, and in a similar way we are lead to define a new total angular momentum $\hat{F} = \hat{I} + \hat{J}$, which commutes with the Hamiltonian of equation (74). For atoms with a $S = 1/2$ ground state like Rb, this leads to a splitting into two hyperfine levels as shown in 9.

Traditionally, most atomic physics experiments have been carried out with the alkali metals which have only one valence electron. However, atoms like Sr and Yb which have two valence electrons are becoming increasingly important. We will look at why this is and some of the differences between one and two electron atoms in the lecture and the homework.

It should also be noted that multi-electron systems are common in solid-state systems such as quantum dots, and the concepts discussed in the homework such as intercombination transitions are very important there also.

7 Atoms in electromagnetic fields

In this section we will very briefly consider the origin of the Hamiltonians that we use commonly use in atomic physics to describe the coupling between atoms and static fields, and between atoms light.

[14] there are exotic systems where this is not true, such as highly ionized heavy atoms

A more detailed treatment is given in Woodgate and Bransden and Joachim. In all cases we will use a semiclassical treatment, where the electromagnetic field is not quantised.

7.1 The interaction Hamiltonian

A general approach[15] to the problem of atoms interacting with electromagnetic fields starts with the scalar and vector potentials ϕ and $\mathbf{A}$. This treatment starts with the general form of the Hamiltonian for a charged particle in and electromagnetic field

$$\hat{H} = \frac{1}{2m}(\hat{p} - q\hat{A})^2 + q\phi \tag{75}$$

from which is its possible to obtain the following approximate Hamiltonian that describes the coupling of a one electron atom to the electromagnetic field

$$\hat{H} = \frac{-i\hbar e}{m}\hat{A} \cdot \hat{\nabla}. \tag{76}$$

If we consider the case of plane polarised electromagnetic waves than the vector potential can be written as

$$\hat{A}(\mathbf{r}, \omega, t) = \hat{\epsilon} A_0(\omega) \left(\exp\left[i(\mathbf{k} \cdot \mathbf{r} - \omega t\right] + \text{c.c.}\right) \tag{77}$$

where $\hat{\epsilon}$ is the polarization unit vector. The matrix elements coupling the ground $|g\rangle$ and excited $|g\rangle$ states therefore have the form $\langle e|e^{-i\mathbf{k}\cdot\mathbf{r}}\hat{\epsilon} \cdot \hat{\nabla}|g\rangle$.

The next step is to expand the exponential

$$e^{-i\mathbf{k}\cdot\mathbf{r}} = 1 + (i\mathbf{k} \cdot \mathbf{r}) + \frac{1}{2!}(i\mathbf{k} \cdot \mathbf{r})^2 + \cdots \tag{78}$$

For the optical transitions that we are interested, the wavelength of light is much larger than the size of the atom, and kr is small. Therefore we retain only the first term in the expansion. This approximation is known as the *electric dipole approximation.*

As you will show in the homework, under this approximation the interaction Hamiltonian can be written as

$$\hat{H} = \hat{D} \cdot \hat{E} \tag{79}$$

where $\hat{D} = e\sum_j \hat{r}_j$ is the atomic dipole operator, and the electric field is written as $\hat{E} = \hat{\epsilon} E \cos(\omega t)$.

7.1.1 Electric dipole selection rules

The selection rules that describe which transitions are allowed in the electric dipole approximation are determined by the angular parts of the electronic wavefunction. I will briefly discuss them here:

Parity The electromagnetic interactions conserves parity. The operator $\hat{r}$ has odd parity. The dipole matrix element can therefore only connect states of opposite parity, in order for parity to be conserved overall.

l From the properties of the angular part of the wavefunctions, one can show that the dipole matrix element is zero unless $\Delta l = \pm 1$.

$\mathbf{m_L}$ Similarly, it can be shown that $\Delta m = 0$ or $\Delta m = \pm 1$ depending on the polarization of the light relative to the projection axis.

Spin The dipole operator does not act on the spin part of the wavefunction, so this remains unchanged.

[15] The approach that I follow here is used by *Bransden and Joachim* and *Woodgate.* An alternative development based on the electric and magnetic fields $\mathbf{E}$ and $\mathbf{B}$ is presented in *Loudon*

7.1.2 Higher order transitions

If the dipole matrix element vanishes, the transition may still occur through higher order processes. Retaining the next term $i(\mathbf{k}\cdot\mathbf{r})$ in the expansion gives rise to *magnetic dipole* and *electric quadrupole transition*. Both terms are of the same order of magnitude and much weaker than an electric dipole transition. Magnetic dipole transitions of this kind are very rare (one example is transitions between the ground state fine structure levels of the halogen atoms). Magnetic dipole transitions can also occur via the coupling of the magnetic field with the electron spin. A very important example of this is the microwave transitions between the hyperfine ground states of the alkali atoms, which are used in atomic clocks. In the optical domain, electric quadrupole transitions are sometimes used in frequency standards, such as the Sr^+ ion [12]. Using trapped ions, electric octupole transitions [13] have even been observed!

7.2 Atoms in static electric and magnetic fields

The same Hamiltonians govern the interaction between atoms and static electric and magnetic fields. Let us look at this on more detail.

7.2.1 Static magnetic fields

It can be shown that (Bransden and Joachim chapter 5) that to a very good approximation, the interaction Hamiltonian for an atom in a static magnetic field is of magnetic dipole form

$$\hat{H}_{\mathrm{B}} = -\frac{\mu_{\mathrm{B}}}{\hbar}(\hat{L}+2\hat{S})\cdot\hat{B} - \frac{\mu_{\mathrm{N}}}{\hbar}\hat{I}\cdot\hat{B} \tag{80}$$

where μ_{B} is the Bohr magneton, and μ_{N} is the nuclear magneton. The operator notation for B reflects the fact that the magnetic field has a direction. The magnetic field couples to the magnetic dipole associated with the orbital angular momentum L and the intrinsic angular momentum S of the electrons. The factor of two in front of the spin is the *gyromagnetic ratio* of the electron which can be calculated using the fully relativistic Dirac equation. There is also a coupling to the nuclear spin I, which is much weaker as $\mu_{\mathrm{N}}/\mu_{\mathrm{B}} = m_{\mathrm{e}}/m_{\mathrm{p}}$. This term can only sometimes be neglected however [16].

7.2.2 Static electric fields

Here once again it is the dipole term

$$\hat{H}_{\mathrm{E}} = \hat{D}\cdot\hat{E} \tag{81}$$

that dominates, as laboratory electric fields do not vary appreciably across the size of the atom. The dipole selection rules apply for the matrix elements, and states with different values of the projection m_J along the field direction are not coupled, as it is impossible to make circularly polarized static fields.

8 Angular momentum operators and matrix elements

The types of problems that you will come across in atomic structure, or the interaction of atoms with static fields, will involve calculating the matrix elements of combinations of angular momentum operators, such as $\hat{I}\cdot\hat{J}$ or $\hat{B}\cdot\hat{S}$. In this section of the course, we will look in more detail at the structure of these calculations and how they can be carried out.

Often, in calculations of atomic structure or atom-field interactions, we are interested in calculating the splitting or shifts of energy levels withiin a single configuration (ie a single value of n and l), where the radial part of the matrix element is the same for all the states concerned. In this case, we need to calculate the angular parts of the matrix elements of operators such as $\hat{I}\cdot\hat{J}$ for the states that we are interested in.

[16] It is after all responsible for all of NMR including its use in medical imaging!

To follow this discussion more easily, let us take a concrete example, which you will solve as part of the lectures. The Hamiltonian governing the Zeeman splitting and hyperfine structure in the ground state of the alkali metals such as Rb can be written as:

$$\hat{H} = A\hat{I}\cdot\hat{J} - 2\mu_B\hat{B}\cdot\hat{S} \tag{82}$$

where we have used the fact that $L = 0$, and neglected the interaction of the nuclear spin with the magnetic field. We will assume that the magnetic field is applied along the z axis, in which case the second term becomes $-2\mu_B B\hat{S}_z$, where S_z is the operator that projects the spin along the magnetic field axis.

8.1 Working in the coupled basis

One way to tackle the problem is to start with the eigenfunctions of $\hat{H}$ at zero magnetic field. In this case, the total angular momentum $\hat{F} = \hat{I} + \hat{J}$ is a good quantum number. For an alkali atom with electronic spin $S = 1/2$, there are thus two eigenstates $F = I + 1/2$ and $F = I - 1/2$. The challenge then is to calculate the matrix elements of the Zeeman Hamiltonian in the F, m_F basis. The matrix elements that we need to calculate have the form $\langle F', m'_F|\hat{S}_z|F, m_f\rangle$. As the operator S_z acts in the S, m_s subspace, we must decompose the $|F, m_F\rangle$ states into the $|S, I, m_s, m_I\rangle$ basis. For example, in the ^{87}Rb ground state where $I = 3/2$ we have

$$|F = 1, m_F = +1\rangle = \left(-\frac{\sqrt{3}}{2}\right)\left|\frac{1}{2}, \frac{3}{2}, -\frac{1}{2}, +\frac{3}{2}\right\rangle + \left(\frac{1}{2}\right)\left|\frac{1}{2}, \frac{3}{2}, +\frac{1}{2}, +\frac{1}{2}\right\rangle \tag{83}$$

where the numerical factors in parenthesis are *Clebsch-Gordan* coefficients. The operator $\hat{S}_z$ can then be applied to each part of the state in turn. The advantages of working in the coupled basis is that you do not necessarily need to be able to write down the full Hamiltonian - only the energies of the states before the field is applied are required. However the angular momentum algebra required can become very complex, particularly when more than one level of decoupling is required (ie when F must be decoupled first into I, J and then again into I, S, L). The first homework uses the coupled basis.

8.2 Working in the uncoupled basis

In the **uncoupled basis** the states are labelled according to their coarse structure quantum numbers n and ℓ and the magnetic quantum number for each component of angular momentum (orbital m_ℓ, electron, m_s, and nuclear, m_I, spin). Thus the state labels are $|n\ell : m_\ell m_s m_I\rangle$ In this basis the atomic Hamiltonian can be written as

$$\hat{H} \;=\; \hat{H}_0 + \hat{H}_{\rm fs} + \hat{H}_{\rm hfs} + \hat{H}' \;, \tag{84}$$

where H_0 is a diagonal matrix consisting of the coarse structure energy levels, $E_{n\ell}$. $H_{\rm fs}$ and $H_{\rm hfs}$ are the fine and hyperfine interactions, and H' is the interaction induced by the external field. Ignoring $H_{\rm fs}$, $H_{\rm hfs}$ and H', each $n\ell$ level has a degeneracy of $D_{n\ell} = (2\ell + 1)(2I + 1)(2s + 1)$, consequently the Hamiltonian for each $n\ell$ level can be written as a sub-matrix of dimension $D_{n\ell} \times D_{n\ell}$. Eigenvalues and eigenvectors of the total Hamiltonian can then be obtained via matrix diagonlisation.

8.2.1 Examples

For $I = 1/2$, $\ell = 0$, e.g. the hydrogen ground state, the unperturbed s-state matrix $H_{\rm s}$ is a 4×4 with elements $\langle i, j|H_0 + H_{\rm fs} + H_{\rm hfs}|i, j\rangle$, where $|i, j\rangle$ are the spin states

$$\left|m_s = +\tfrac{1}{2}, m_I = +\tfrac{1}{2}\right\rangle \;=\; |+,+\rangle \;, \tag{85}$$

$|+,-\rangle$, $|-,+\rangle$, and $|-,-\rangle$. Similarly, for $\ell = 1$, $H_{\rm p}$ is a 12×12 where the four spin components are repeated for each m_ℓ state.

The advantage of this method is that it is not necessary to carry out lengthy angular momentum algebra, and the physics of each interaction can be introduced in a straightforward way. The disadvantage is that knowledge of the complete fine and hyperfine Hamiltonians is needed, rather than just the eigenenergies. In addition, the hamiltonian rapidly becomes too large to construct and manipulate analytically, so computer methods should be used.

The coupled basis is therefore useful for analytic calculations, or where the exact details of the fine and hyperfine operators are not known. The uncoupled basis lends itself to exact numerical calculations for large groups of states on a computer. The next section details how such calculations in the uncoupled basis can be carried out in practice, and in the homework you will apply these techniques to the calculation of the Breit-Rabi diagram for Rb.

9 Angular problems in the uncoupled basis: the Breit-Rabi diagram

This section of the notes introduces the techniques that you need for performing calculations in the uncoupled basis using a computer. We will illustrate the technique by calculating the behaviour of the ^{87}Rb hyperfine levels in a magnetic field. These notes and the computer codes were developed by Prof. Charles Adams.

9.1 Spin matrices

To construct the fine and hyperfine interaction matrices in the uncoupled basis we use the standard techniques for adding angular momenta. The first step is to write down the spin matrices for an arbitrary angular momentum j.

All angular momentum operators satisfy the same set of commutation rules and we can derive the general result (for an arbitrary angular momentum j, see e.g. Ballantyne, p. 121)

$$\hat{j}_+|j,m\rangle \;=\; \sqrt{j(j+1)-m(m+1)}|j,m+1\rangle \;,$$

where $\hat{j}_+ = \hat{j}_x + i\hat{j}_y$. Consequently the matrix $\hat{j}_+$ is only non-zero along the upper diagonal with elements $\sqrt{j(j+1)-m(m+1)}$, e.g. for $j=\frac{3}{2}$ we have (note that it is the m value along the top that is used to calculate the matrix element):

$$\begin{array}{c|cccc} & \frac{3}{2} & \frac{1}{2} & -\frac{1}{2} & -\frac{3}{2} \\ \frac{3}{2} & 0 & \sqrt{3} & 0 & 0 \\ \frac{1}{2} & 0 & 0 & \sqrt{4} & 0 \\ -\frac{1}{2} & 0 & 0 & 0 & \sqrt{3} \\ -\frac{3}{2} & 0 & 0 & 0 & 0 \end{array} \;.$$

$\hat{j}_-$ is given by the transpose of $\hat{j}_+$, and

$$\begin{aligned} \hat{j}_x &= \tfrac{1}{2}(\hat{j}_+ + \hat{j}_-) \;, \\ \hat{j}_y &= -\tfrac{i}{2}(\hat{j}_+ - \hat{j}_-) \;, \\ \hat{j}_z &= \tfrac{1}{2}(\hat{j}_+\hat{j}_- - \hat{j}_-\hat{j}_+) \;. \end{aligned}$$

Using these results one can construct a function (e.g. for matlab the function spin.m[17] is given below) that returns the matrix components for any spin or angular momenta.

[17]
```
function s=spin(j)
d=2*j+1; m=j-1:-1:-j; jm=sqrt(j*(j+1)-m.*(m+1));
sp=full(sparse(1:d-1,2:d,jm,d,d));
sm=full(sparse(2:d,1:d-1,jm,d,d));
s=(sp+sm)/2;s(:,:,2)=(-sp+sm)*i/2;
s(:,:,3)=(sp*sm-sm*sp)/2;
```

9.2 Adding angular momenta

Once we have built the matrices for an arbitrary angular momentum it is easy to add two or more angular momentum. The components of the sum of two angular momenta, e.g., j_1 and j_2, in matrix form are given by

$$\hat{J}_i = \hat{j}_{1i} \otimes \mathbb{1}_{2j_2+1} + \mathbb{1}_{2j_1+1} \otimes \hat{j}_{2i} \ ,$$

where $\mathbb{1}_{2j+1}$ is a unity matrix with dimension $2j+1$. First we will do one example analytically for the simplest case of two spin$-\frac{1}{2}$s, (e.g. the ^{1}H ground state), and then develop a general method for any state. This approach offers an alternative insight to the standard Clebsch-Gordan, 3-j and 6-j symbol formulism.

9.2.1 Two spin$-\frac{1}{2}$s.

Consider two spin$-\frac{1}{2}$ particles (labelled 1 and 2). Each particle may be either in the 'spin-up' state, $|\uparrow\rangle$ or the 'spin-down' state, $|\downarrow\rangle$. We write the wavefunction of the first spin as $|\psi\rangle_1 = a_1|\uparrow\rangle + b_1|\downarrow\rangle$, and similarly for the second. We can also write this as a vector,

$$|\psi\rangle_1 = \begin{pmatrix} a_1 \\ b_1 \end{pmatrix} \ , \text{ and } |\psi\rangle_2 = \begin{pmatrix} a_2 \\ b_2 \end{pmatrix} \ .$$

The combined state of the two spins is

$$|\psi\rangle = |\psi\rangle_1 \otimes |\psi\rangle_2 = a_1a_2|\uparrow\uparrow\rangle + a_1b_1|\uparrow\downarrow\rangle + a_2b_1|\downarrow\uparrow\rangle + a_2b_2|\downarrow\downarrow\rangle$$

or in vector notation

$$|\psi\rangle = \begin{pmatrix} a_1 \\ b_1 \end{pmatrix} \otimes \begin{pmatrix} a_2 \\ b_2 \end{pmatrix} = \begin{pmatrix} a_1a_2 \\ a_1b_2 \\ b_1a_2 \\ b_1b_2 \end{pmatrix} \ ,$$

where $\otimes$ is a tensor product (make copies of the second matrix with positions and prefactors given by the first). An operator in this 4-dimensional vector space is given by a 4×4 matrix. We want to construct the operator corresponding to the total angular momentum. The angular momentum of a spin$-\frac{1}{2}$ (in units of $\hbar$) is $\hat{\boldsymbol{J}} = \frac{1}{2}\hat{\boldsymbol{\sigma}}$, where $\hat{\boldsymbol{\sigma}} = (\hat{\sigma}_x, \hat{\sigma}_y, \hat{\sigma}_z)$ is a 'spinor' with components equal to the Pauli spin matrices. The total angular momentum is given by the sum of the contributions from each particle,

$$\hat{\boldsymbol{J}} \ = \ \tfrac{1}{2}(\hat{\boldsymbol{\sigma}}_1 \otimes \mathbb{1}_2 + \mathbb{1}_2 \otimes \hat{\boldsymbol{\sigma}}_2) \ , \tag{86}$$

where $\mathbb{1}_2$ is a 2×2 unity matrix. Note that the operator order specifies which term acts on which spin: e.g. $\hat{\sigma} \otimes \mathbb{1}_2$ means that we apply $\hat{\sigma}$ to the first particle and the identity matrix (i.e. do nothing) to the second; whereas $\mathbb{1}_2 \otimes \hat{\sigma}_x$ means do nothing to the first particle and apply $\hat{\sigma}_x$ to the second.

To construct the matrix for $\hat{\boldsymbol{J}}^2$ consider each component separately,

$$\begin{aligned}
\hat{J}_x &= \tfrac{1}{2}(\hat{\sigma}_x \otimes \mathbb{1}_2 + \mathbb{1}_2 \otimes \hat{\sigma}_x) \qquad (87)\\
&= \tfrac{1}{2}\left[\begin{pmatrix} 0 & 1 \\ 1 & 0 \end{pmatrix} \otimes \begin{pmatrix} 1 & 0 \\ 0 & 1 \end{pmatrix} + \begin{pmatrix} 1 & 0 \\ 0 & 1 \end{pmatrix} \otimes \begin{pmatrix} 0 & 1 \\ 1 & 0 \end{pmatrix}\right] \\
&= \tfrac{1}{2}\begin{pmatrix} 0 & 1 & 1 & 0 \\ 1 & 0 & 0 & 1 \\ 1 & 0 & 0 & 1 \\ 0 & 1 & 1 & 0 \end{pmatrix}, \\
\hat{J}_y &= \tfrac{1}{2}(\hat{\sigma}_y \otimes \mathbb{1}_2 + \mathbb{1}_2 \otimes \hat{\sigma}_y) \\
&= \tfrac{1}{2}\left[\begin{pmatrix} 0 & -i \\ i & 0 \end{pmatrix} \otimes \begin{pmatrix} 1 & 0 \\ 0 & 1 \end{pmatrix} + \begin{pmatrix} 1 & 0 \\ 0 & 1 \end{pmatrix} \otimes \begin{pmatrix} 0 & -i \\ i & 0 \end{pmatrix}\right] \\
&= \tfrac{1}{2}\begin{pmatrix} 0 & -i & -i & 0 \\ i & 0 & 0 & -i \\ i & 0 & 0 & -i \\ 0 & i & i & 0 \end{pmatrix}, \qquad (88)\\
\hat{J}_z &= \tfrac{1}{2}(\hat{\sigma}_z \otimes \mathbb{1}_2 + \mathbb{1}_2 \otimes \hat{\sigma}_z) \\
&= \tfrac{1}{2}\left[\begin{pmatrix} 1 & 0 \\ 0 & -1 \end{pmatrix} \otimes \begin{pmatrix} 1 & 0 \\ 0 & 1 \end{pmatrix} + \begin{pmatrix} 1 & 0 \\ 0 & 1 \end{pmatrix} \otimes \begin{pmatrix} 1 & 0 \\ 0 & -1 \end{pmatrix}\right] \\
&= \tfrac{1}{2}\begin{pmatrix} 2 & 0 & 0 & 0 \\ 0 & 0 & 0 & 0 \\ 0 & 0 & 0 & 0 \\ 0 & 0 & 0 & -2 \end{pmatrix}. \qquad (89)
\end{aligned}$$

Next, we square the matrices[18]

$$\begin{aligned}
\hat{J}_x^2 &= \tfrac{1}{4}\begin{pmatrix} 0 & 1 & 1 & 0 \\ 1 & 0 & 0 & 1 \\ 1 & 0 & 0 & 1 \\ 0 & 1 & 1 & 0 \end{pmatrix}\begin{pmatrix} 0 & 1 & 1 & 0 \\ 1 & 0 & 0 & 1 \\ 1 & 0 & 0 & 1 \\ 0 & 1 & 1 & 0 \end{pmatrix} \\
&= \tfrac{1}{2}\begin{pmatrix} 1 & 0 & 0 & 1 \\ 0 & 1 & 1 & 0 \\ 0 & 1 & 1 & 0 \\ 1 & 0 & 0 & 1 \end{pmatrix}.
\end{aligned}$$

[18] We could have avoided squaring a 4×4 matrix by making use of $\hat{\sigma}_x^2 = \mathbb{1}$ and $\hat{\sigma}_{x1} = \hat{\sigma}_{x2} = \hat{\sigma}_x$, to rearrage (87) as

$$\begin{aligned}
\hat{J}_x^2 &= \tfrac{1}{4}(\hat{\sigma}_x \otimes \mathbb{1} + \mathbb{1} \otimes \hat{\sigma}_x)^2 \\
&= \tfrac{1}{4}(\hat{\sigma}_x^2 \otimes \mathbb{1} + \hat{\sigma}_x \otimes \hat{\sigma}_x + \hat{\sigma}_x \otimes \hat{\sigma}_x + \mathbb{1} \otimes \hat{\sigma}_x^2) \\
&= \tfrac{1}{2}(\mathbb{1} \otimes \mathbb{1} + \hat{\sigma}_x \otimes \hat{\sigma}_x)\,,
\end{aligned}$$

Substituting

$$\hat{\sigma}_x \otimes \hat{\sigma}_x = \begin{pmatrix} 0 & 1 \\ 1 & 0 \end{pmatrix} \otimes \begin{pmatrix} 0 & 1 \\ 1 & 0 \end{pmatrix} = \begin{pmatrix} 0 & 0 & 0 & 1 \\ 0 & 0 & 1 & 0 \\ 0 & 1 & 0 & 0 \\ 1 & 0 & 0 & 0 \end{pmatrix},$$

we obtain,

$$\hat{J}_x^2 = \tfrac{1}{2}(\mathbb{1} \otimes \mathbb{1} + \hat{\sigma}_x \otimes \hat{\sigma}_x) = \tfrac{1}{2}\begin{pmatrix} 1 & 0 & 0 & 1 \\ 0 & 1 & 1 & 0 \\ 0 & 1 & 1 & 0 \\ 1 & 0 & 0 & 1 \end{pmatrix}.$$

Similarly,

$$\hat{J}_y^2 = \tfrac{1}{2}\begin{pmatrix} 1 & 0 & 0 & -1 \\ 0 & 1 & 1 & 0 \\ 0 & 1 & 1 & 0 \\ -1 & 0 & 0 & 1 \end{pmatrix},$$

$$\hat{J}_z^2 = \tfrac{1}{2}\begin{pmatrix} 2 & 0 & 0 & 0 \\ 0 & 0 & 0 & 0 \\ 0 & 0 & 0 & 0 \\ 0 & 0 & 0 & 2 \end{pmatrix},$$

and the total angular momentum

$$\hat{\boldsymbol{J}}^2 = \hat{J}_x^2 + \hat{J}_y^2 + \hat{J}_z^2 = \begin{pmatrix} 2 & 0 & 0 & 0 \\ 0 & 1 & 1 & 0 \\ 0 & 1 & 1 & 0 \\ 0 & 0 & 0 & 2 \end{pmatrix}.$$

To find the eigenvalues we put

$$\begin{vmatrix} 2-\lambda & 0 & 0 & 0 \\ 0 & 1-\lambda & 1 & 0 \\ 0 & 1 & 1-\lambda & 0 \\ 0 & 0 & 0 & 2-\lambda \end{vmatrix} = 0 .$$

which gives

$$(2-\lambda)^2(\lambda^2 - 2\lambda) = 0 ,$$

giving three eigenvalues with $\lambda = 2$ and one with $\lambda = 0$. As the eigenvalues of the total angular momentum are $J(J+1)$, these correspond to $J = 1$ and $J = 0$, respectively. For $\lambda = 0$

$$\begin{pmatrix} 2 & 0 & 0 & 0 \\ 0 & 1 & 1 & 0 \\ 0 & 1 & 1 & 0 \\ 0 & 0 & 0 & 2 \end{pmatrix}\begin{pmatrix} a \\ b \\ c \\ d \end{pmatrix} = 0 ,$$

which gives $a = d = 0$ and $c = -b$, i.e., the eigenvector is

$$|0,0\rangle = \tfrac{1}{\sqrt{2}}\begin{pmatrix} 0 \\ 1 \\ -1 \\ 0 \end{pmatrix},$$

where we have used the label $|j,m\rangle$ for the eigenvector, with m being the eigenvalues of $\hat{J}_z$. We will verify the m quantum numbers below. For $\lambda = 2$

$$\begin{pmatrix} 0 & 0 & 0 & 0 \\ 0 & -1 & 1 & 0 \\ 0 & 1 & -1 & 0 \\ 0 & 0 & 0 & 0 \end{pmatrix}\begin{pmatrix} a \\ b \\ c \\ d \end{pmatrix} = 0 ,$$

so either $a = 1$, $b = c = d = 0$, or $a = d = 0$ and $b = c$, or $d = 1$, $a = b = c = 0$, i.e., the eigenvectors are

$$|1,1\rangle = \begin{pmatrix} 1 \\ 0 \\ 0 \\ 0 \end{pmatrix}, \; |1,0\rangle = \tfrac{1}{\sqrt{2}}\begin{pmatrix} 0 \\ 1 \\ 1 \\ 0 \end{pmatrix}, \text{ and } |1,-1\rangle = \begin{pmatrix} 0 \\ 0 \\ 0 \\ 1 \end{pmatrix}.$$

What about $\hat{J}_z$? Using (89) we find

$$\begin{aligned}\hat{J}_z|1,1\rangle &= \begin{pmatrix}1&0&0&0\\0&0&0&0\\0&0&0&0\\0&0&0&-1\end{pmatrix}\begin{pmatrix}1\\0\\0\\0\end{pmatrix}\\ &= 1\begin{pmatrix}1\\0\\0\\0\end{pmatrix} = 1|1,1\rangle\ .\end{aligned}$$

Similarly, $\hat{J}_z|1,-1\rangle = -1|1,-1\rangle$, $\hat{J}_z|1,0\rangle = 0$, and $\hat{J}_z|0,0\rangle = 0$.

For the hydrogen ground state the total angular momentum is labelled as F and its projection as m_F. By finding the eigenvectors of the total angular momentum matrix $\hat{F}^2$, we have related the eigenstates in the *coupled basis*, labelled $|F, m_F\rangle$ (which also happens to the eigenbasis of the hyperfine interaction), to those in the *uncoupled basis* $|m_I, m_s\rangle$. This relationship between the coupled and uncoupled states is shown in the lower half of Fig. 10

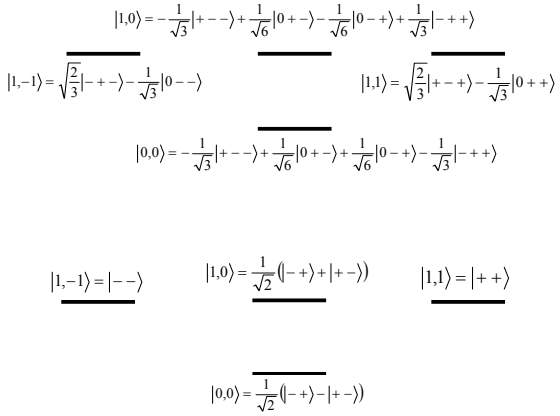

Figure 10: The decomposition of the ${}^2S_{1/2}$ (lower) and ${}^2P_{1/2}$ (upper) $|F, m_F\rangle$ states in terms of the uncoupled states, $|m_I, m_s\rangle$ or $|m_\ell, m_I, m_s\rangle$, for a nuclear spin $I = 1/2$.

9.2.2 A spin$-\frac{1}{2}$ and a spin-1.

In this case, we are not adding the angular momentum of two separate particles, but different contributions to the same particle, however the addition works in the same way, i.e., for the x-component, we write

$$\hat{J}_x = \hat{L}_x \otimes \mathbb{1}_{2S+1} + \mathbb{1}_{2L+1} \otimes \hat{S}_x\ ,$$

where $\hat{S}_x = \frac{1}{2}\hat{\sigma}_x$, $\mathbb{1}_{2S+1}$ and $\mathbb{1}_{2L+1}$ means do nothing to the S and L parts of the wavefunction, respectively. Using the spin commutation relations, Section 9.1 we find that

$$\begin{aligned}\hat{L}_x &= \frac{1}{\sqrt{2}}\begin{pmatrix}0&1&0\\1&0&1\\0&1&0\end{pmatrix}, \hat{L}_y = \frac{1}{\sqrt{2}}\begin{pmatrix}0&-i&0\\i&0&-i\\0&i&0\end{pmatrix}\ ,\\ \hat{L}_z &= \begin{pmatrix}1&0&0\\0&0&0\\0&0&-1\end{pmatrix}\ .\end{aligned}$$

As $\hat{L}_z$ has eigenvalues $1, 0, -1$ we now have 6 basis states,

$$|\psi\rangle = a|{+}{+}\rangle + b|{+}{-}\rangle + c|0{+}\rangle + d|0{-}\rangle + e|{-}{+}\rangle + f|{-}{-}\rangle\ ,$$

using the labelling $|m_\ell, m_s\rangle$. Writing out the 6×6 matrices is too much like hard work so we resort to our favourite software (matlab or mathematica). You should verify that the matrix for the total angular momentum is

$$\hat{J}^2 \;=\; \begin{pmatrix} \frac{15}{4} & 0 & 0 & 0 & 0 & 0 \\ 0 & \frac{7}{4} & \sqrt{2} & 0 & 0 & 0 \\ 0 & \sqrt{2} & \frac{11}{4} & 0 & 0 & 0 \\ 0 & 0 & 0 & \frac{11}{4} & \sqrt{2} & 0 \\ 0 & 0 & 0 & \sqrt{2} & \frac{7}{4} & 0 \\ 0 & 0 & 0 & 0 & 0 & \frac{15}{4} \end{pmatrix} .$$

As expected this has two eigenvalues of $\frac{3}{4}$ and four of $\frac{15}{4}$. The eigenvectors are

$$\begin{aligned} |\tfrac{1}{2},-\tfrac{1}{2}\rangle &= -\sqrt{\tfrac{2}{3}}|{-}{+}\rangle + \sqrt{\tfrac{1}{3}}|{0}{-}\rangle \\ |\tfrac{1}{2},+\tfrac{1}{2}\rangle &= -\sqrt{\tfrac{2}{3}}|{+}{-}\rangle + \sqrt{\tfrac{1}{3}}|{0}{+}\rangle \\ |\tfrac{3}{2},-\tfrac{1}{2}\rangle &= -\sqrt{\tfrac{2}{3}}|{0}{-}\rangle - \sqrt{\tfrac{1}{3}}|{-}{+}\rangle \\ |\tfrac{3}{2},+\tfrac{1}{2}\rangle &= \sqrt{\tfrac{2}{3}}|{0}{+}\rangle + \sqrt{\tfrac{1}{3}}|{+}{-}\rangle \\ |\tfrac{3}{2},-\tfrac{3}{2}\rangle &= |{-}{-}\rangle \quad \text{and} \quad |\tfrac{3}{2},+\tfrac{3}{2}\rangle = |{+}{+}\rangle \; . \end{aligned}$$

9.2.3 Adding nuclear spin.

Once we have added L and S to form J we can add the nuclear spin in the same way, i.e.,

$$\hat{F}_x \;=\; \hat{J}_x \otimes \mathbb{1}_{2I+1} + \mathbb{1}_{2J+1} \otimes \hat{I}_x \; ,$$

etc. For the $^2P_{1/2}$ state, we find that the hyperfine sub-levels $|F, m_F\rangle$ can be written as the following superpositions

$$\begin{aligned} |0,0\rangle &= -\tfrac{1}{\sqrt{3}}|{+}{-}{-}\rangle + \tfrac{1}{\sqrt{6}}|{0}{+}{-}\rangle + \tfrac{1}{\sqrt{6}}|{0}{-}{+}\rangle - \tfrac{1}{\sqrt{3}}|{-}{+}{+}\rangle \\ |1,-1\rangle &= \sqrt{\tfrac{2}{3}}|{-}{+}{-}\rangle - \tfrac{1}{\sqrt{3}}|{0}{-}{-}\rangle \\ |1,0\rangle &= -\tfrac{1}{\sqrt{3}}|{+}{-}{-}\rangle + \tfrac{1}{\sqrt{6}}|{0}{+}{-}\rangle - \tfrac{1}{\sqrt{6}}|{0}{-}{+}\rangle + \tfrac{1}{\sqrt{3}}|{-}{+}{+}\rangle \\ |1,+1\rangle &= \sqrt{\tfrac{2}{3}}|{+}{-}{+}\rangle - \tfrac{1}{\sqrt{3}}|{0}{+}{+}\rangle \; . \end{aligned}$$

This decomposition is illustrated in the upper half of Fig. 1.

9.2.4 Decomposition for an arbitrary angular momentum state

By finding the eigenvectors of the $\hat{F}^2$ matrix we can write any state in the coupled $|F, m_F\rangle$ basis in terms of its uncoupled components. As the matrices can become very large we will do this numerically. One of the problems is that a standard eigenvalue algorithm cannot order degenerate eigenstates so we do not know which state is which. To solve this problem we find the eigenvectors of a matrix where all the degeneracy is lifted by a combination of fine, hyperfine and 'pseudo'–Zeeman splitting. In fact if we use the operator

$$\hat{H} \;=\; 2(2I+1)\hat{H}_{\rm fs} + 2\hat{H}_{\rm hfs} + \hat{F}_z + \tfrac{1}{2}(g_F+1) \; , \tag{90}$$

where $g_F = (2\ell+1)(2I+1)(2S+1)$ is the total degeneracy, the eigenvalues are integers in the range 1 to g_F and the eigenvectors are ordered according to their value of J, F and m_F. Below[19] is a matlab program to determine the eigenvector of a specified $|F, m_F\rangle$ level for a given I, L, S, and J.

[19] function ev=evec2(is,l,s,j,f,m)
SS=spin(s);Sx=SS(:,:,1);Sy=SS(:,:,2);Sz=SS(:,:,3);

9.3 Transition amplitudes

For electric dipole transitions, the spin state remains unchanged, so to calculate a transition strength we look for the amount of a particular spin configuration in the initial and final states. For example, recalling that for $^2S_{1/2}$ we found

$$|0,0\rangle \;=\; \tfrac{1}{\sqrt{2}}(|{+-}\rangle - |{-+}\rangle)\;|1,0\rangle = \tfrac{1}{\sqrt{2}}(|{+-}\rangle + |{-+}\rangle)\;,$$

we see (Fig. 10) that there are contributions from both the $|{+-}\rangle$ and $|{-+}\rangle$ to the $F, m_F = 0 \rightarrow F', m'_F = 0$ transitions. For $F = F'$, the two contributions cancels, whereas for $F \neq F'$ they add to give $\sqrt{\frac{1}{3}}$. To find the transition amplitude between an initial state $|\ell, m_\ell, F, m_F\rangle$ and a final state $|\ell \pm 1, m_\ell \pm q, F', m'_F\rangle$ we calculate the projection $\langle \ell \pm 1, m_\ell \pm q, F', m'_F | \ell, m_\ell, F, m_F\rangle$, where $|\ell, m_\ell, F, m_F\rangle$ is a reduced eigenvector only containing the terms with a particular ℓ and m_ℓ.[20] An example showing electric dipole couplings for the coupled and uncoupled bases is shown in Fig. 11.

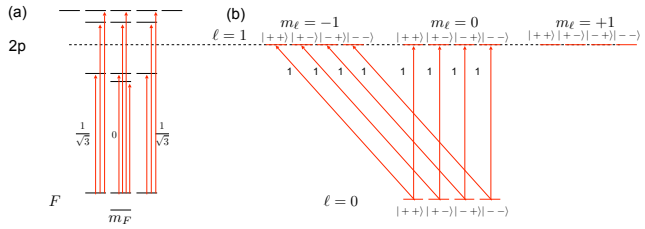

Figure 11: The different couplings for electric dipole transitions in the (a) coupled and (b) uncoupled basis. To obtain the transition amplitudes for the coupled basis we write the coupled states in the uncoupled basis and calculate the overlap or projection of the appropriate ℓ m_ℓ sections of the initial and final states.

```
gs=2*s+1;Si=eye(gs);
LL=spin(l);Lx=LL(:,:,1);Ly=LL(:,:,2);Lz=LL(:,:,3);
gl=2*l+1;Li=eye(gl);
II=spin(is);Ix=II(:,:,1);Iy=II(:,:,2);Iz=II(:,:,3);
gi=2*is+1;Ii=eye(gi);
Jx=kron(Lx,Si)+kron(Li,Sx);
Jy=kron(Ly,Si)+kron(Li,Sy);
Jz=kron(Lz,Si)+kron(Li,Sz);
gj=gl*gs;Ji=eye(gj);
J2=kron(Jx*Jx+Jy*Jy+Jz*Jz,Ii);
fx=kron(Jx,Ii)+kron(Ji,Ix);
fy=kron(Jy,Ii)+kron(Ji,Iy);
fz=kron(Jz,Ii)+kron(Ji,Iz);
gf=gj*gi;Fi=eye(gf);
f2=fx*fx+fy*fy+fz*fz;
hs=f2-is*(is+1)*Fi-J2;
fs=J2-(l*(l+1)+s*(s+1))*Fi;
split=hs+(2*is+1)*fs+fz+(gf+1)/2*Fi;
[V,D]=eig(split);
id=f*(f+1)-is*(is+1)-j*(j+1)+(2*is+1)*(j*(j+1)-l*(l+1)-s*(s+1))+m+(gf+1)/2;
ev=V(:,id);
```

[20] function cg=cleb2(is,l1,j1,f1,m1,l2,j2,f2,q)
if abs(m1+q)>f2
cg=0;
else
gvec=evec2(is,l1,1/2,j1,f1,m1);
lg=length(gvec);
evec=evec2(is,l2,1/2,j2,f2,m1+q);
le=length(evec);
lm=(le-lg)/2;lp=(le+lg)/2;
revec=evec(lm*(1-q)+1:lp-lm*q);
cg=gvec'*revec;
end

9.4 Project: - The Breit-Rabi diagram

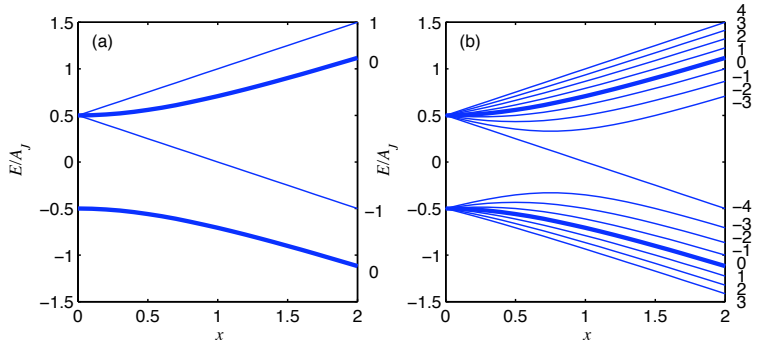

Figure 12: A plot of the Zeeman shift of the hyperfine sublevels (or Breit-Rabi diagram) for (a) ^{1}H and (b) ^{133}Cs. Here $x = g_J \mu_B B/A$.

As an application of these techniques, you will calculate the Breit-Rabi diagram for the ground state of ^{87}Rb using both the coupled and the uncoupled basis. Doing the calculation two ways will allow you to check the answer, and also provide you with more insight into the nature of these calculations and the differences between the various methods.

The Breit-Rabi diagram is a plot of the energy shift of the hyperfine sublevels in a magnetic field. Examples for ^{1}H and ^{133} Cs are shown in Fig 12. More details are given on the homework sheet.

References

[1] M. P. A. Jones *et al.*, Phys. Rev. A **75**, 040301 (R) (2007).

[2] For an accessible discussion of pure and mixed states and the density matrix, see *Density matrix theory and applications*, by K. Blum (Plenum 1996).

[3] A. H. Myerson *et al.*, Phys. Rev. Lett, **100**, 200502 (2008).

[4] B. Darquié *et al.*, Science **309**, 454 (2005).

[5] J. Gea-Banacloche, *et al.,* Phys. Rev. A, **51** 576, (1995).

[6] M. Fleischhauer *et al.*,, Rev. Mod. Phys. **77** 633–673 (2005).

[7] H. R. Gray and C. R. Stroud, Opt. Comm. **25** 359 (1978).

[8] K. Bergmann *et al.*, Rev. Mod. Phys. **70**, 1003 (1998).

[9] E. Brion, L. H. Pedersen, and K. Mølmer, Journal of Physics A **40** 1033 (2007).

[10] T. F. Gallager, *Rydberg Atoms*, Cambridge University Press (1994).

[11] D. Steck, ^{87}*Rb D line data*, http://steck.us/alkalidata/

[12] H. S. Margolis *et al.*, Science **306**, 1355 (2004).

[13] M. Roberts *et al.*, Phys. Rev. Lett. **78**, 1876 (1997).